

FORAMINIFERAL BIOSTRATIGRAPHY AND PALAEOENVIRONMENTAL ANALYSIS OF THE MID-CRETACEOUS LIMESTONES IN THE SOUTHERN TIBETAN PLATEAU

MARCELLE K. BOUDAGHER-FADEL^{1,4}, XIUMIAN HU², G. DAVID PRICE¹, GAOYUAN SUN², JIAN-GANG WANG³ AND WEI AN²

ABSTRACT

This study of mid-Cretaceous foraminifera from the Linzhou, the Coqen and the Xigaze Basins in the southern Tibetan Plateau has provided the first high resolution biostratigraphic description of these limestones and interpretation of their paleoenvironmental settings. The fossil assemblages are dominated primarily by orbitolinid larger benthic foraminifera. We reassessed the identification of many taxa, dividing the South Tibetan sedimentary successions of Aptian to Early Cenomanian age into eight new foraminiferal biozones (TLK1 a–h): (i) (TLK1a) a shallow reefal environment corresponding to planktonic foraminifera zone (PZ) Aptian 1–2, dominated by *Palorbitolina* and *Praeorbitolina* spp.; (ii) (TLK1b) a transgressive, reefal to forereefal environment corresponding to PZ Aptian 3, characterized by the first appearance of *Mesorbitolina parva*; (iii) (TLK1c) a shallow reefal to backreef environment of Late Aptian (PZ Aptian 4) age, characterized by the first appearance of *Mesorbitolina texana*; (iv) (TLK1d) a transgressive phase of forereef to an inner neritic environment of Albian (PZ Albian 1) age, characterized by the first appearance of *Cuneolina pavonia*; (v) (TLK1e) an open-marine reefal environment of Albian (PZ Albian 2) age, with assemblages dominated by flat to slightly conical orbitolinids, characterized by the first appearance of *Palorbitolinoides hedini*; (vi) (TLK1f) a shallow, open-marine reefal to forereef environment of Middle Albian (PZ Albian 3) age, dominated by flat and convex orbitolinids, and characterized by the first appearance of *Mesorbitolina aperta*; (vii) (TLK1g) a reefal to forereef environment of end Albian (PZ Albian 4) age, characterized by the appearance of *Conicorbitolina* cf. *cuvillieri* and *Pseudochoffatella cuvillieri*, and in which Early Aptian species of *Praeorbitolina* cf. *wienandsi* have been recorded for the first time from the Late Albian; (viii) (TLK1h) a shallow reefal environment of Early Cenomanian age characterized by the first appearance of *Conicorbitolina* sp. A and *Nezzazata conica*. The eight new biozones provided biostratigraphic correlation of the Langshan, Sangzugang and Takena Formations in the Lhasa terrane, while the observed evolution of the environmentally controlled microfacies corresponds closely with the current, inferred global sea-level variation of the period. The almost continuous sedimentary sequences studied allowed previously defined orbitolinid phylogenetic lineages to be confirmed.

INTRODUCTION

In the mid-Cretaceous (93–126 Ma), modern day southern Tibet was paleogeographically located at the southern margins of the Asian Plate bordering the eastern Tethyan Ocean. It was the site for the deposition of large volumes of sub-tropical backreef and reefal, shallow-marine carbonates. The variations in foraminiferal assemblages, in particular the larger benthic foraminiferal (LBF) assemblages, are essential for dating the mid-Cretaceous limestones in southern Tibet and understanding the paleoenvironmental and tectonic development of the region. At this time, the LBF assemblages in the region were dominated mainly by agglutinated orbitolinids.

Although studies of the mid-Cretaceous Tibetan orbitolinids have been reported over the last four decades (e.g., Zhang, 1982, 1986, 2000; Smith & Xu, 1988; Yin et al., 1988; Zhang et al., 2004) from isolated occurrences, their detailed biostratigraphy is not available. Also, the taxonomy and identification schemes used are often not compatible with the now widely accepted description of orbitolinids (see Schroeder et al., 2010).

In this study, we describe orbitolinid-rich assemblages from largely continuous sedimentary sequences from the Lhasa terrane of the southern Tibetan Plateau, which range in age from Early Aptian to Early Cenomanian. Material from the Sangzugang Formation from the Xigaze Basin, the Takena Formation in the Linzhou Basin, the Langshan Formation in the Coqen Basin were analyzed in this study (Fig. 1).

GEOLOGICAL SETTING

The Tibetan Plateau (Fig. 1) comprises a series of terranes, including (from north to south) the Songpan-Ganzi complex, the Qiangtang terrane, and the Lhasa terrane (Yin & Harrison, 2000). The Lhasa terrane, located on the southern part of the Tibetan Plateau, is bounded by the Yarlung-Zangbo suture zone with the Tethyan Himalaya to the south, and by the Bangong-Nujiang suture zone with the Qiangtang terrane to the north (Yin & Harrison, 2000; Zhu et al., 2013). The Lhasa terrane is divided into southern, central and northern subterrane, which are separated by the Luobadui-Milashan Fault (LMF) and the Shiquan River-Nam Tso Mélange Zone (SNMZ), respectively (Zhu et al., 2011, 2013).

The southern Lhasa subterrane is comprised of the Gangdese magmatic arc and Xigaze forearc basin. The Gangdese magmatic arc is characterized by Late Triassic-Early Paleogene Gangdese batholiths and Paleogene Linzizong volcanic rocks, with minor sedimentary cover (Chu et al., 2006; Ji et al., 2009; Zhu et al., 2013). The Xigaze forearc basin, located in the south of the Gangdese arc (Fig. 1), is dominated by the thick Albian-Campanian deep-water turbidites and thin shallow-marine Sangzugang limestones

¹ Department of Earth Sciences, UCL, Gower Street, London, WC1E 6BT, UK

² School of Earth Sciences and Engineering, Nanjing University, Xianlin Street 163, Nanjing 210023, China

³ Institute of Geology and Geophysics, Chinese Academy of Sciences, Beijing 100029, China

⁴ Correspondence author. E-mail: m.fadel@ucl.ac.uk

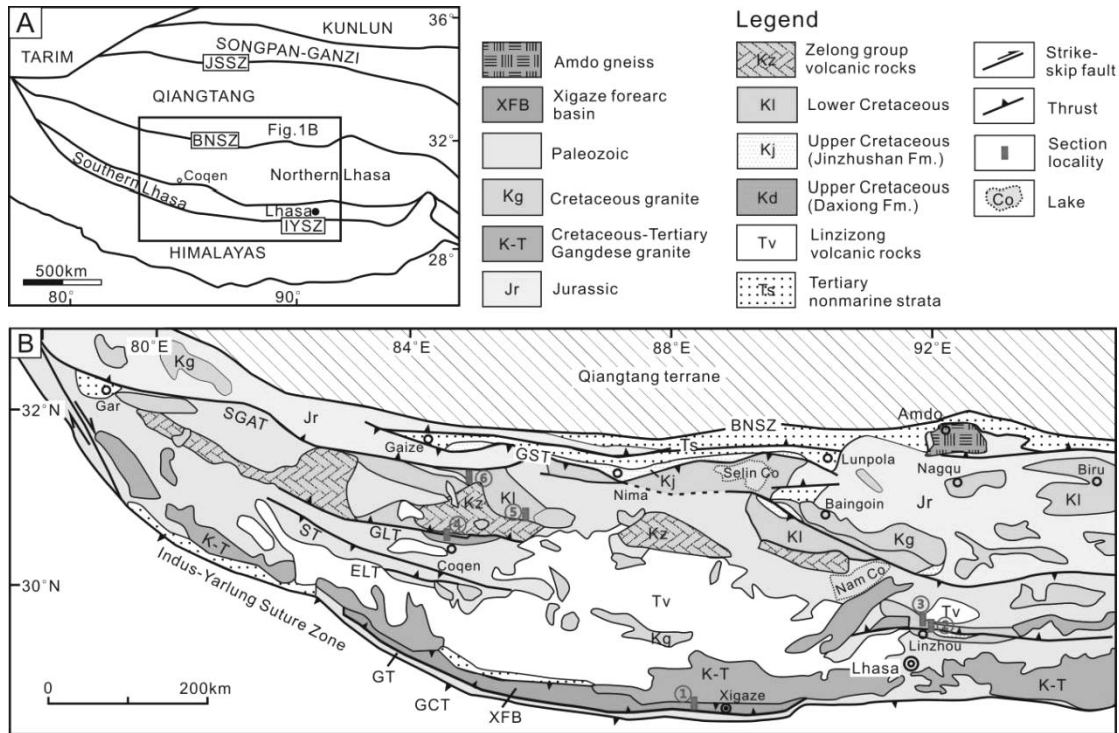


FIGURE 1. **A** Simplified tectonic map of the Tibetan Plateau and adjacent regions, showing the Lhasa terrane in the context of the Tibetan Plateau (Pan et al., 2004). JSSZ—Jinsha suture zone; BNSZ—Bangong-Nujiang suture zone; IYSZ—Indus-Yarlung suture zone. **B** Simplified geological map of the Lhasa terrane modified from Kapp et al. (2005). SGAT—Shiquan-Gaize-Amdo thrust; GST—Gaize-Selin Co thrust; GLT—Gugu La thrust; ST—Shibalu thrust; ELT—Emei La thrust; GT—Gangdese thrust system; GCT—Great Counter thrust. Section 1 from the Xigaze Basin; Sections 2 and 3 from the Linzhou Basin; Sections 4, 5 and 6 from the Coqen Basin.

(Dürr, 1996; Wang & Liu, 1999; Wang et al., 2012; An et al., 2014). The Sangzugang Formation, exposed discontinuously from Sangzugang village in Sagya County to the Xigaze airport, consists of thick-bedded or massive dark-gray bioclastic limestones with abundant benthic foraminifera, rudists and corals, and minor occurrences of bivalves. The 60–230 m thick unit is in fault contact with either the overlying deep-water turbidites or the post-collisional Gangrinboche conglomerate (Wang et al., 2013), and its original stratigraphic relationships are uncertain. The Sangzugang Formation was deposited in reefal environments along the northern part of the forearc basin during the Late Aptian to Early Albian (Liu et al., 1988).

The Linzhou basin lies at the retro-side of the Gangdese arc, and is filled by Jurassic to Cretaceous volcanic, carbonate and terrigenous clastic rocks that are overlain by the Paleogene Linzizong volcanic successions (Pan et al., 2004). The Early Cretaceous Takena Formation in this basin is intercalated between the underlying shore-face Chumulong Formation and the overlying fluvial Shexing Formation (Leier et al., 2007). Orbitolinid-bearing limestone beds occur in the middle of the Takena Formation. Samples from two sections (the Jiarong and Laxue sections) were studied.

In the central Lhasa subterrane, Carboniferous metasedimentary deposits, Permian limestones, Jurassic siliciclastic deposits and abundant Cretaceous magmatic and sedimentary rocks are widespread in many places. In our study area

(Fig. 1), thick (up to several km) Cretaceous sedimentary strata are exposed (Pearce & Mei, 1988; Harris et al., 1990; Zhu et al., 2009, 2011). These strata are composed of the Lower Cretaceous Duoni sedimentary-volcanic rocks, the Langshan limestone, and Upper Cretaceous Daxiong continental molasse (Leeder et al., 1988; Yin et al., 1988; Zhang, 2000; Zhang et al., 2004; Sun et al., 2015). The Langshan limestone, upon which this study focused, is exposed in a west-east direction, extends up to ~1000 km in the central Lhasa subterrane, and is bounded by the Gangdese magmatic arc to the south and Shiquan River-Nam Tso Mélange Zone Gaize-Selin Co thrust (SNMZGST) to the north (Zhang, 2000; Zhang et al., 2004; Kapp et al., 2007).

LITHOSTRATIGRAPHY AND SAMPLING

The Sangzugang Formation in the Xigaze Basin is 60 to 230 m thick (Fig. 2), and it outcrops near the northern boundary of the Xigaze forearc basin (Wang et al., 2012; An et al., 2014). Based on foraminiferal data, the Sangzugang section (GPS: 29°18'11.1"N, 88°24'51.3"E) has been dated as Aptian–Albian in age (Cherchi & Schroeder, 1980; Bassoulet et al., 1984).

In the Linzhou basin, the Penbo Member of the Takena Formation (Yin et al., 1988; Leier et al., 2007) consists of about 250 m of mudstone, siltstone and limestone with overlying successions of fluvial red beds of the Shexing Formation. Previous studies placed the Takena limestones as

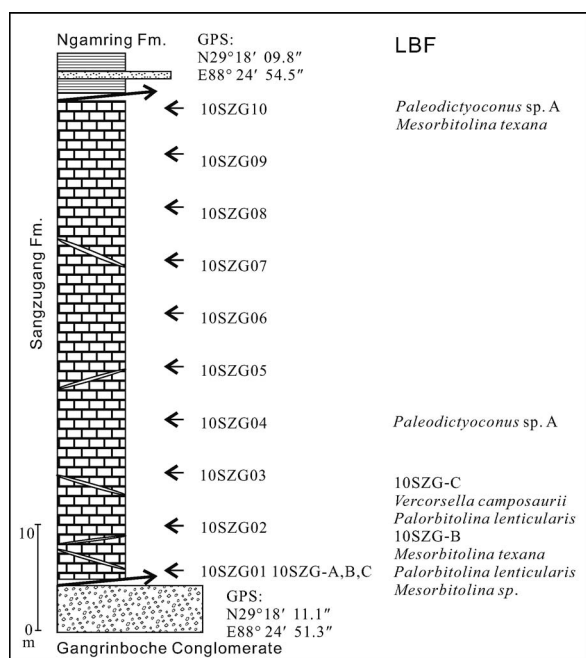


FIGURE 2. Stratigraphy of the Sangzugang Formation in the Sangzugang section, Xigaze Basin, showing the samples' position and occurrence of main LBF of biozone TLK1c.

Aptian–Late Albian based upon the study of echinoids, ammonoids and foraminifera (Yin et al., 1988). In this study, we measured and sampled the limestone-bearing strata (a ~100 m thick middle part of the Takena Formation) from two sections: the Jiarong section ($29^{\circ}53'48.7''\text{N}$, $91^{\circ}19'19.1''\text{E}$) and the Laxue section ($29^{\circ}54'25.1''\text{N}$, $91^{\circ}20'48.1''\text{E}$). Detailed lithostratigraphic logs and sample positions are shown in Figure 3.

In the Coqen Basin, the Langshan limestone (Fig. 1) unconformably overlies volcanic rocks of the Lower Cretaceous Zelong Group or conformably overlies the Duoni Formation (see Sun et al., 2015), and is mainly composed of ~80–800 m of orbitolinid-bearing wackestones and packstones (XZBGM, 1993; Zhang et al., 2004; Scott et al., 2010). Three sections of mid-Cretaceous Langshan limestones were measured and sampled for this study. The Langshan Formation in the Azhang section ($31^{\circ}56'48.5''\text{N}$, $84^{\circ}55'16.5''\text{E}$) consists of ~800 m of orbitolinid-rich limestones (Fig. 4), while the Langshan Formation in the Guolong section ($31^{\circ}26'23.6''\text{N}$, $85^{\circ}24'46.6''\text{E}$) reaches ~400 m in thickness (Fig. 5), and the Xiagezi section ($31^{\circ}10'52.0''\text{N}$, $84^{\circ}52'14.0''\text{E}$) consists of ~80 m of orbitolinid-bearing wackestones and packstones (Fig. 6).

In total, our study is based on a detailed analysis of over 350 samples from six logged stratigraphic sections (see Figs. 2–6). Analyses of these samples allowed us to review the mid-Cretaceous Tibetan benthic foraminiferal assemblages and to revise their stratigraphic range, while tracing their phylogenetic and paleoenvironmental evolution, which correlates well with the current inferred global sea-level variation of the period (Fig. 7). The occurrence of planktonic foraminifera (PF) at some levels of the sections allowed us to constrain

the ages of these LBF and to confirm the dating of the formations.

TIBETAN ORBITOLINIDS: TAXONOMY, PHYLOGENETIC EVOLUTION AND BIOZONATION

During the deposition of the mid-Cretaceous sediments of the Takena, Langshan and Sangzugang Formations, agglutinated foraminifera made up the bulk of the foraminiferal assemblages, while PF were sporadic, only occurring at a few levels. Small biserial/triserial textularids, conical cuneolinids (e.g., *Cuneolina*, *Vercorsella*, *Sabaudia*) and planispiral forms (e.g., *Pseudocyclammina*) are common. However, the major components of these formations are the flat to broadly conical orbitolinids.

The orbitolinids are characterized by conical tests that are usually a few millimeters in height and diameter (although they can attain diameters of 5 cm or more). In axial section, the embryo is located at the apex of the cone, followed by a series of discoidal chamber layers. In transverse section, the chambers are seen divided into a marginal zone, with subepidermal partitions and a central zone with radial partitions. The radial partitions in *Orbitolina* thicken away from the periphery and anastomose in the central area, producing an irregular network. The earliest formed chambers of the megalospheric generation can form a complex embryonic apparatus that can be divided into a protoconch, deuteroconch, a subembryonic zone and periembryonic chamberlets depending on the genera involved. For instance, in *Palorbitolina*, the embryonic apparatus consists of a large, globular, fused protoconch and deuteroconch, followed by periembryonic chambers. *Praeorbitolina* evolved an embryonic apparatus divided into a protoconch and deuteroconch with an incompletely divided subembryonic zone. In *Mesorbitolina*, the deuteroconch and subembryonic zone are more or less of equal thickness. In *Conicorbitolina*, the marginal zone becomes extensively divided by vertical and horizontal partitions, while in *Orbitolina* the deuteroconch is highly subdivided and of much greater thickness than the subembryonic zone (Fig. 8; see Schroeder, 1975; Hottinger, 1978; Simmons et al., 2000; BouDagher-Fadel, 2008; Schroeder et al., 2010).

During this study, we redefined many of the orbitolinid species previously defined by Zhang (1982, 1986, 1991) from Xainsa, Baingoin and western Tibet as synonyms of previously established species. Some of Zhang's species were revised by Rao et al. (2015).

SYSTEMATIC PALEONTOLOGY

Order FORAMINIFERIDA Eichwald, 1830
 Superfamily ORBITOLINOIDEA Martin, 1890
 Family ORBITOLINIDAE Martin, 1890
 Genus *Palorbitolina* Schroeder, 1961

Type species: *Madreporites lenticularis* Blumenbach, 1805

Palorbitolina lenticularis (Blumenbach, 1805)

Fig. 9.1

Madreporites lenticularis, Blumenbach, 1805 p. 80, figs. 1–6.

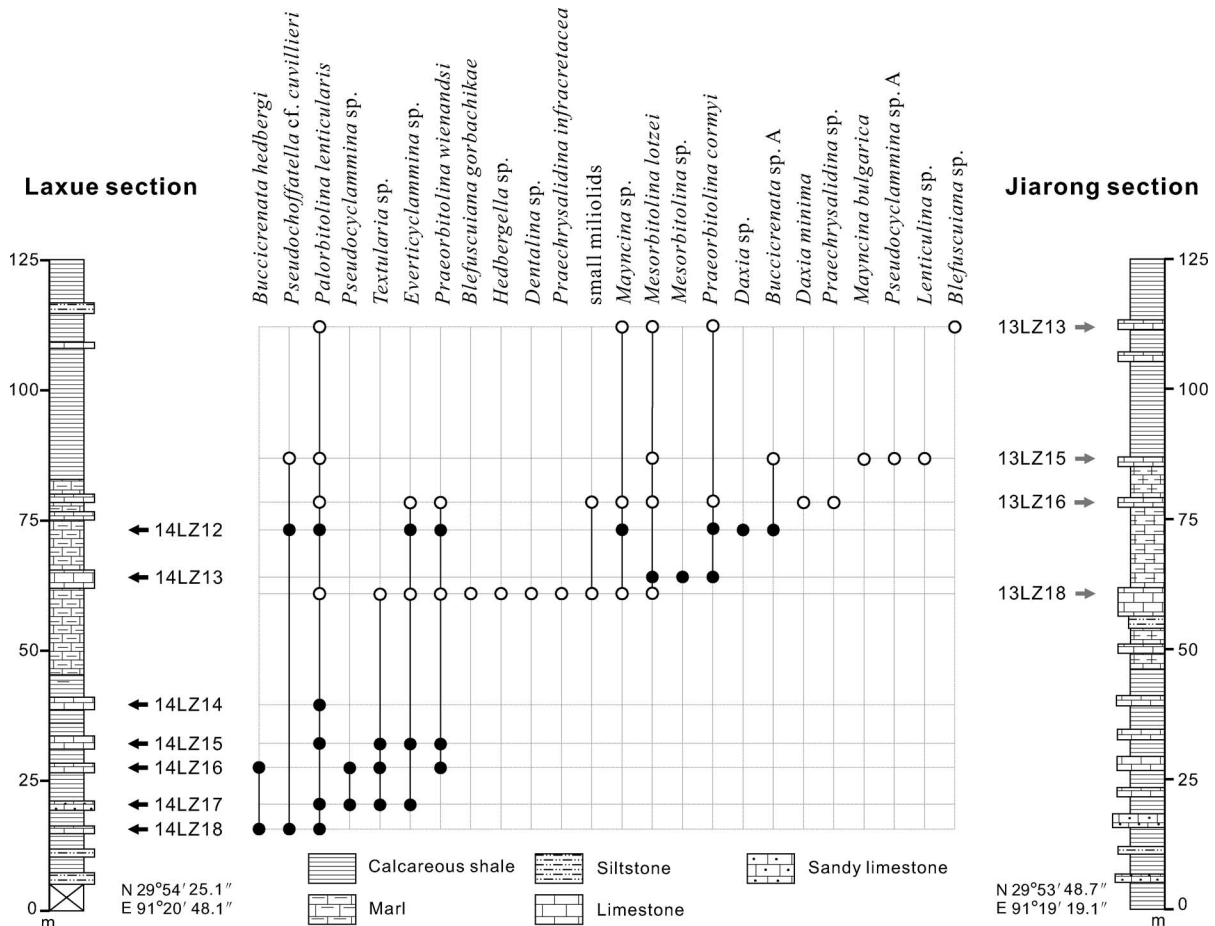


FIGURE 3. Stratigraphy of the Takena Formation in the Jiarong and Laxue sections, Liuzhou basin, showing the samples' position and occurrence of LBF. Black circles are samples from the Laxue section, while white circles are from the Jiarong section.

Orbitolina (Palorbitolina) discoidea Gras, Zhang, 1982, pl. 8, figs. 1–10, pl. 7, fig. 10.

Orbitolina (Palorbitolina) umbellata Zhang, 1982, pl. 7, fig. 15.

Orbitolina (Palorbitolina) complanata Zhang, 1982, pl. 8, figs. 13–17, pl. 9, figs. 1–7.

Discussion. *Palorbitolina lenticularis* is characterized by an annular periembryonic zone completely surrounding the upper part of the centric embryonic chamber. It was described as *O. (P.) umbellata* and *O. (P.) complanata* from the Aptian of Takena Formation in Xizang, China.

Distribution. This species is found in this study in the Aptian (PZ Aptian 1–4a, TLK1a–early part of TLK1c) in Jiarong, Laxue, Azhang and Guolong sections and in the Linzhou basin.

Genus *Mesorbitolina* Schroeder, 1962

Type species: *Orbitulites texanus* Roemer, 1849

Mesorbitolina birmanica (Sahni, 1937)

Fig. 9.10

Orbitolina birmanica Sahni, 1937, p. 368, pl. 30, figs. 1–19.

Orbitolina (Mesorbitolina) birmanica Sahni, Zhang, 1986, p. 112, pl. 5, figs. 1–2.

Orbitolina (Orbitolina) deltoidea Zhang, 1982, p. 73, pl. 12, fig. 7.

Discussion. *Mesorbitolina birmanica* is characterized by a biconvex embryonic apparatus, which includes a plano-convex protoconch and a deuteroconch that is irregularly subdivided by occasional partitions. Zhang (1982) described *O. (O.) deltoidea*, which is similar to *M. birmanica*, as new species from the lower Cretaceous of the Lhasa Block of Tibet.

Distribution. In this study, *M. birmanica* was found in the Aptian to Albian (PZ Aptian 4–Albian 4, TLK1c–g) in Azhang, Guolong sections and in the Coqen basin.

Mesorbitolina lotzei Schroeder, 1964

Orbitolina (Mesorbitolina) lotzei Schroeder, 1964, p. 469, text-fig. 3a–f.

Orbitolina (Columnorbitolina) tibetica Cotter, Zhang, 1982, pl. 2, figs. 7–16.

Discussion. This species is characterized by a centrally positioned embryo, laterally surrounded by an annular first postembryonic chamber. Zhang (1982) illustrated similar

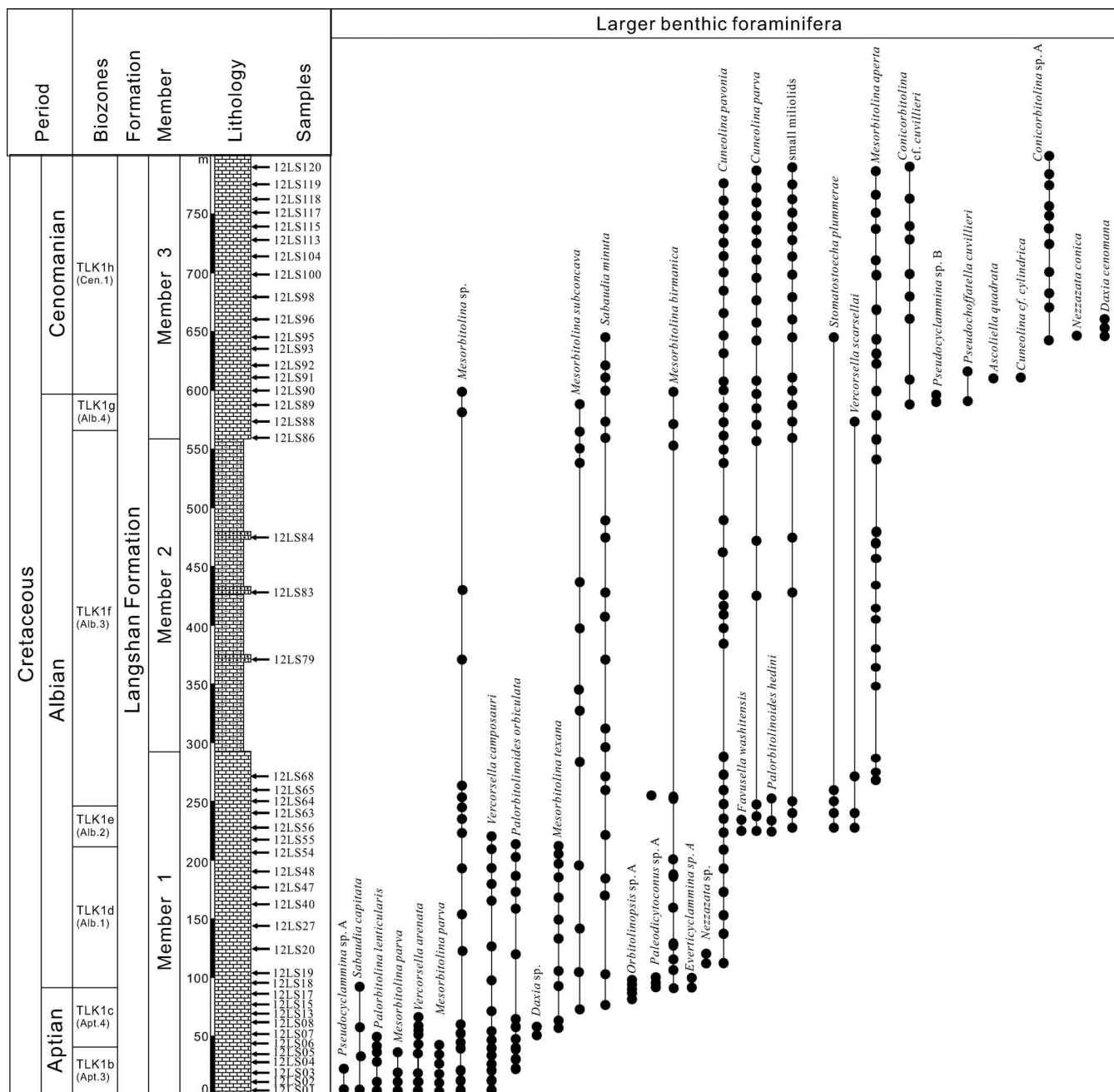


FIGURE 4. Stratigraphy of the Langshan Formation in the Azhang section, Coqen basin, showing the sample positions and occurrence of LBF.

forms from the lower Cretaceous of the Lhasa Block of Tibet under his new genus and identified them as *Orbitolina* (*Columnorbitolina*) *tibetica*. Here, this species is considered to be a synonym of *M. lotzei*.

Distribution. This species is here found in Aptian age (PZ Aptian 2, upper part of TLK1a) sections of Jiarong and Laxue, and in the Linzhou basin.

Mesorbitolina parva (Douglas, 1960)
Figs. 10.1, 10.3

Orbitolina parva Douglas, 1960, p. 39, pl. 9, figs. 1–14.

Orbitolina (*Columnorbitolina*) *lhuenzhubensis* Zhang, 1982, p.74, pl. 3, figs. 6–9.

Orbitolina (*Columnorbitolina*) *minuscula* Zhang, 1982, pl. 6, figs. 5–9.

Orbitolina (*Columnorbitolina*) *parva* Douglas, Zhang, 1982, pl. 3, figs. 10–13.

Orbitolina (*Columnorbitolina*) *scitula* Zhang 1982, p. 64, pl. 4, figs. 6–12.

Orbitolina (*Columnorbitolina*) *absidata* Zhang, 1986, p.109, pl. 2, figs. 13–17.

Mesorbitolina irregularis Zhang, 1986, p. 75, pl. 2, figs. 2–4.

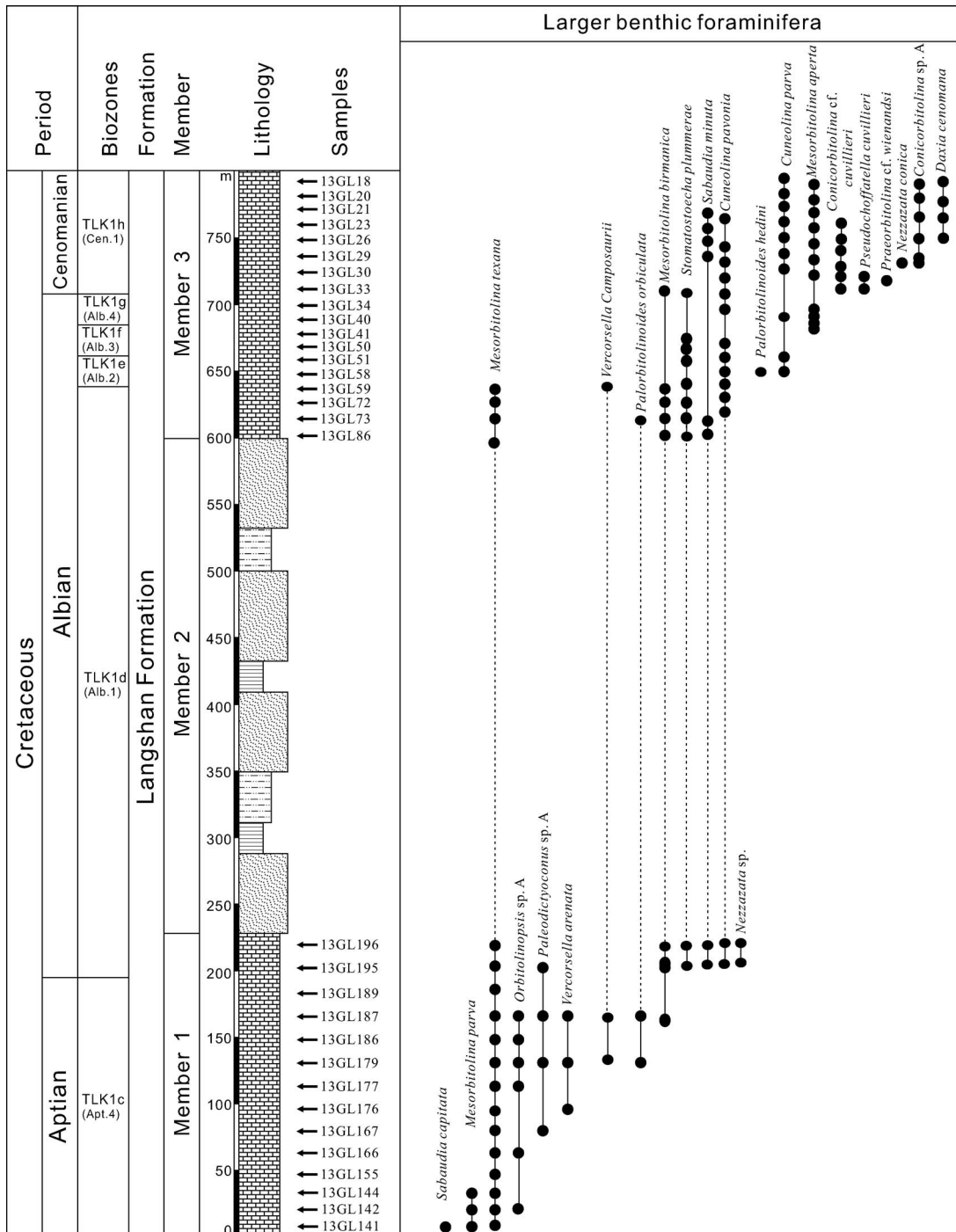


FIGURE 5. Stratigraphy of the Langshan Formation in the Guolong section, Coqen basin, showing specific, labelled sample positions and occurrence of main LBF.

Discussion. This species is characterized by a deuteroconch showing a complete system of radial partitions. Zhang (1982) and (1986) described and illustrated similar forms as new species: *O. (C.) lhuenzhubensis*, *O. (C.) minuscula* and *O. (C.) scitula* from the Aptian of Takena Formation in Xizang, China; *O. (C.) absidata* and *M. irregularis* from the Aptian of the Lhasa Block, Tibet.

Distribution. This species was found in Aptian sections (PZ Aptian 3–4a, TLK1b–TLK1c) of the Azhang, Guolong and Xiagezi in the Coqen basin.

Mesorbitolina texana (Roemer, 1849)
Figs. 10.2, 10.4–10.5

Orbitulites texallus Roemer, 1849, p. 392.

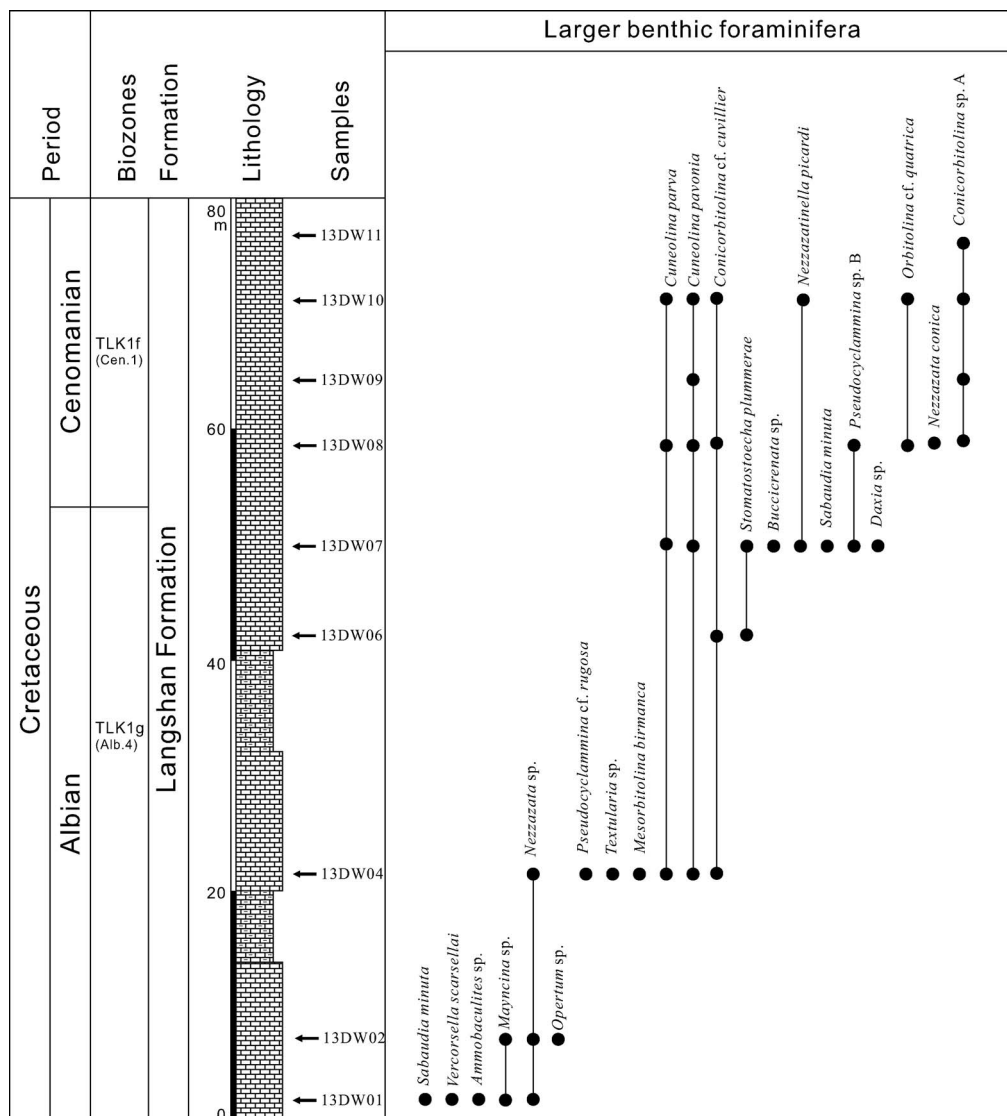


FIGURE 6. Stratigraphy of the Langshan Formation in the Xiagezi section, Coqen basin, showing the sample positions and the distribution of main species of LBF.

- Orbitulites texallus* Roemer, Roemer, 1852, p. 86, fig. 7a–d.
Mesorbitolina maryoensis Zhang, 1982, p.111, pl. 4, figs. 1–6.
Mesorbitolina regularis Zhang, 1986, p. 75, pl. 2, figs. 5–6.
Orbitolina (Palorbitolina) megasphaerica, Zhang, 1982, p. 69, pl. 8, fig. 11.
Orbitolina (Columnorbitolina) orientala Zhang, 1982, p. 65, pl. 6, figs. 1–4.
Orbitolina (Columnorbitolina) pengboensis Zhang, 1982, p. 74, pl.3, figs. 1–5.
Orbitolina (Columnorbitolina) rutogensis, Zhang, 1982, p. 64, pl. 5, figs. 1–15.
Orbitolina (Mesorbitolina) cotyliformis, Zhang, 1982, p. 115, pl. 5, fig. 4.
Orbitolina (Orbitolina) sp., 1986, p. 116, pl. 7, fig. 11.
Orbitolina (Mesorbitolina) texana (Roemer), Zhang, 1986, p. 111, pl. 4, figs. 7–17.

Discussion. This species is characterized by an almost square embryonic apparatus, with clear deuteroconch and sub-embryonic zone, each divided by radial partitions. Zhang (1982, 1986) described a number of new species similar to *M. texana* (see list of synonyms) from the Aptian of Takena Formation in Xizang, China.

Distribution. This species is found in this study in the Aptian to Albian (PZ Aptian 4a–Albian 1, TLKc–TLK1d) of Azhang, Guolong sections and in the Coqen basin.

Mesorbitolina subconcava (Leymerie, 1878)
 Figs. 10.6, 11.5

- Orbitolina subconcava* Leymerie, 1878, pl. E, fig. 7.
Orbitolina (Orbitolina) bangoonica Zhang, 1982, p. 73, pl. 12, figs. 1–6.
Orbitolina (Mesorbitolina) aspera Zhang, 1986, p. 112, pl. 5, figs. 7–9.

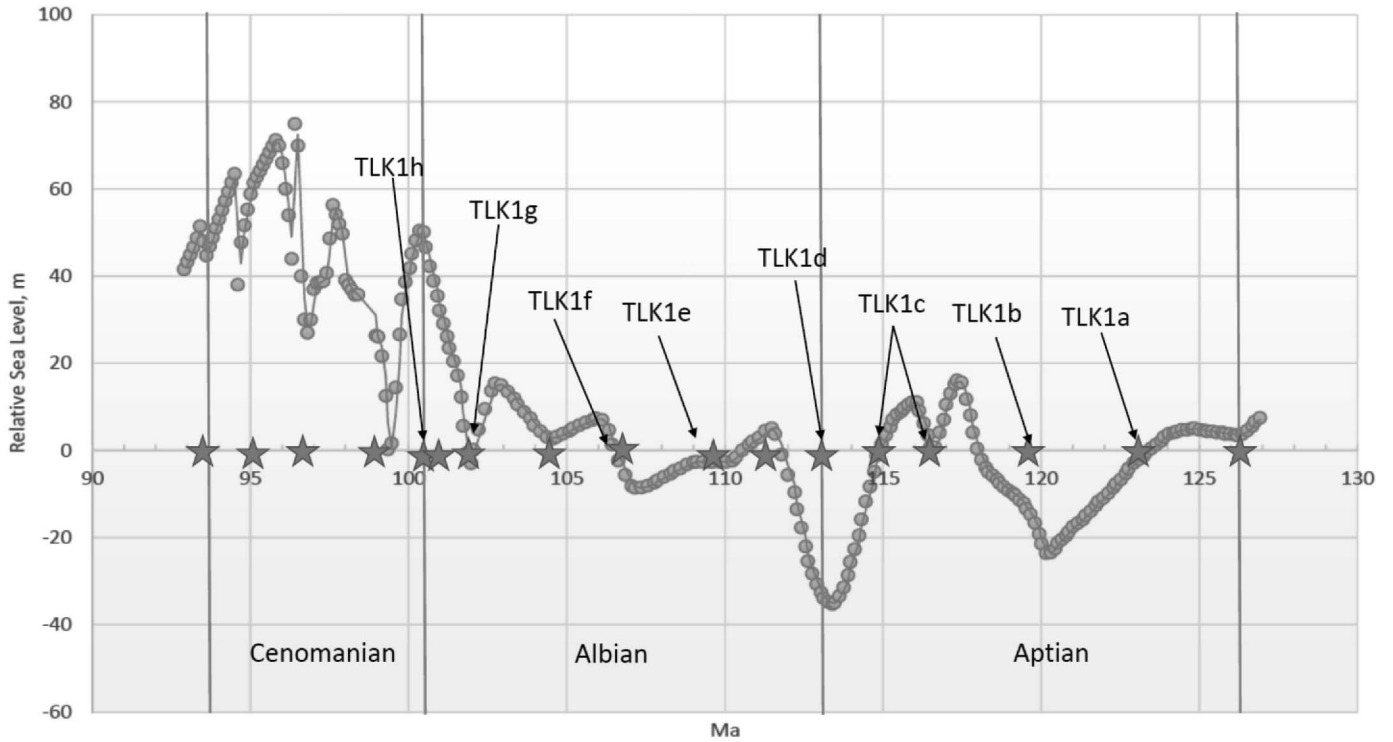


FIGURE 7. Variation in sea-level during the mid-Cretaceous based on Miller et al. (2011). The stars indicate the boundaries of the PZ after BouDagher-Fadel (2013).

Orbitolina (Mesorbitolina) imparilis Zhang, 1986, pl. 6, figs. 5–10.
Orbitolina (Mesorbitolina) langshanensis Zhang, 1986, p. 113, pl. 8, figs. 1–5.

Orbitolina (Mesorbitolina) xainzaensis Zhang, 1986, p. 114, pl. 7, figs. 6–7.
 Discussion. *Mesorbitolina subconcava* is characterized by an oval proloculus surrounded by a well-divided deutero-

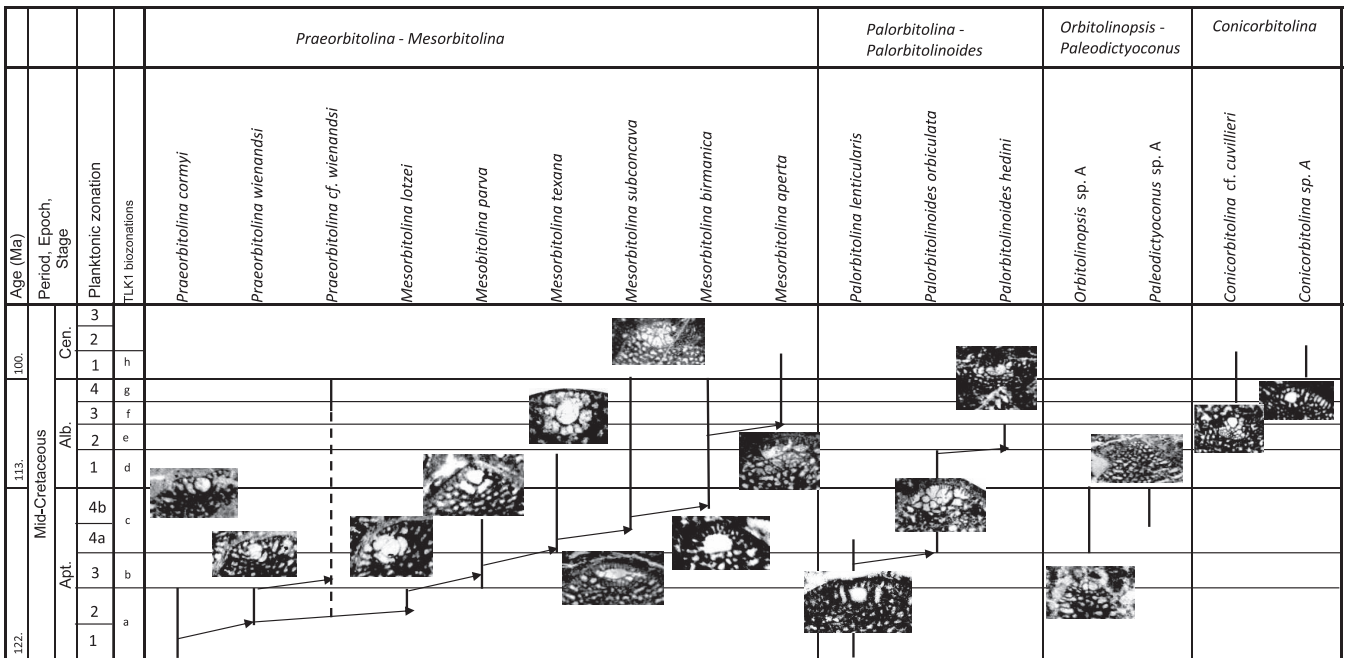


FIGURE 8. Phylogenetic evolution of Tibetan orbitolinids. Planktonic Zones after BouDagher-Fadel (2013).

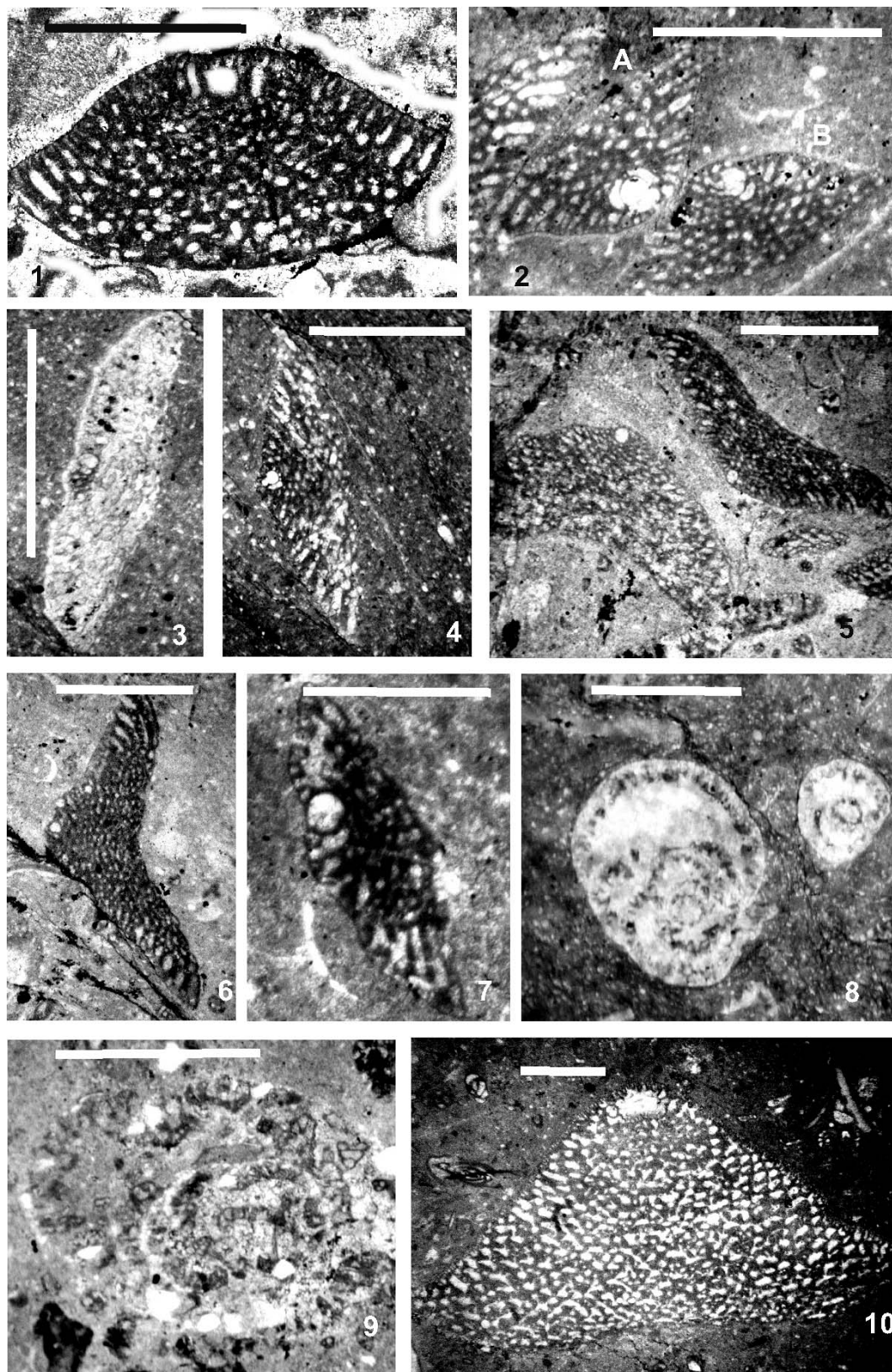


FIGURE 9. **1** *Palorbitolina lenticularis* (Blumenbach), Jiarong section, TLK1a, PZ Aptian 2, sample 14LZ13. **2 A** *Praeorbitolina wienandsi* Schroeder, **B** *Praeorbitolina cormyi* Schroeder, Jiarong section, TLK1a, PZ Aptian 2, sample 14LZ13. **3-7** *Praeorbitolina cormyi*, Jiarong section, 3, 7, TLK1a, PZ Aptian 2, sample 13LZ16, 4-6, Laxue section, TLK1a, PZ Aptian 2, sample 14 LZ12. **8** *Pseudocyclammia* sp. A, Jiarong section, TLK1a, PZ Aptian 2, sample 13LZ15. **9** *Pseudochoffatella* cf. *cuvillieri* Deloffre, A form. Note that the coarsely agglutinated hypodermis has small *Textularia* spp. and small benthic foraminifera incorporated into the wall, Laxue section, TLK1a, PZ Aptian 2, sample 14LZ18. **10** *Mesorbitolina birmanica* (Sahni), Guolong section, TLK1g, PZ Albanian 4, sample 13GL40. Scale bars = 1 mm.

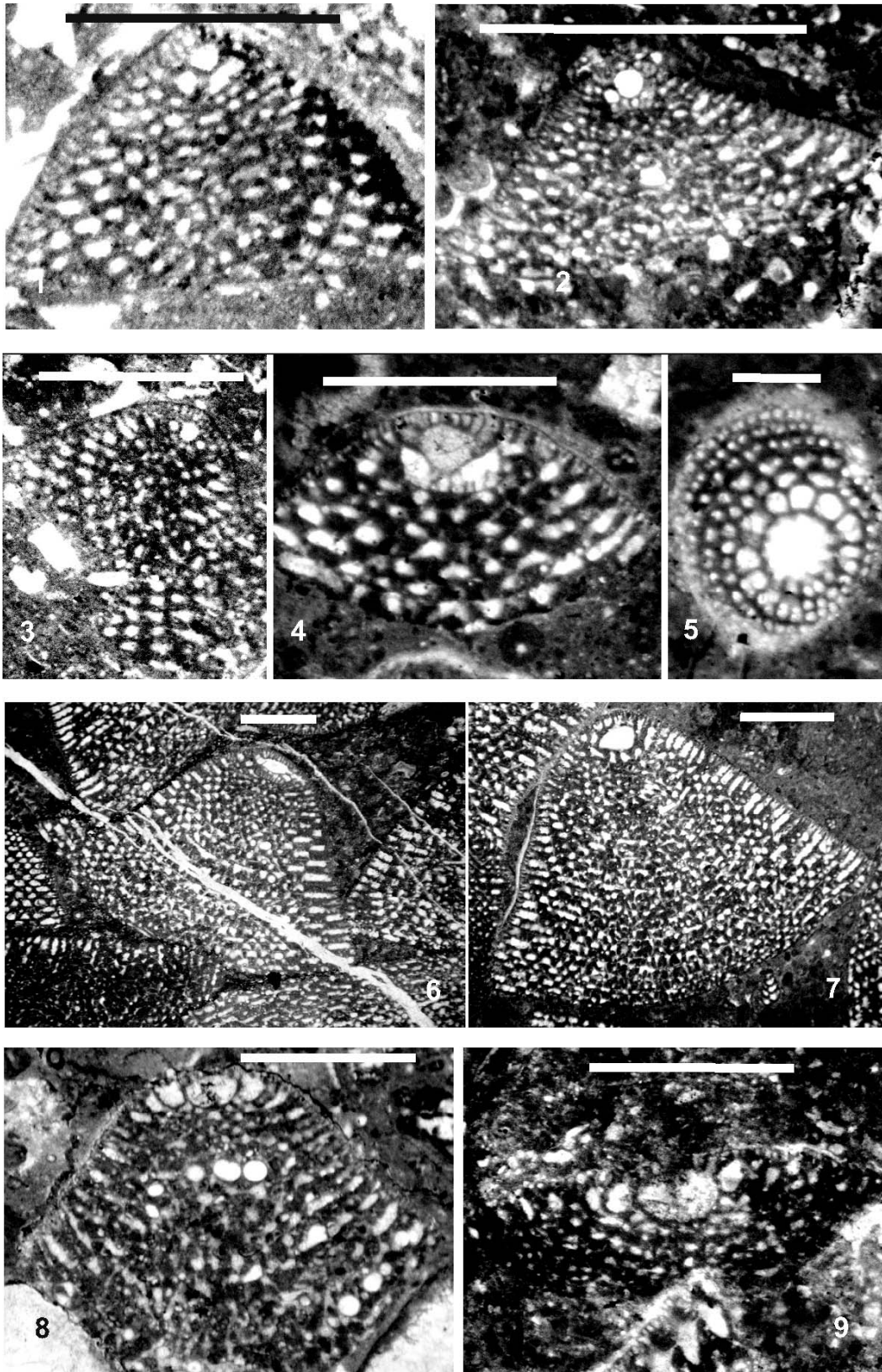


FIGURE 10. 1, 3 *Mesorbitolina parva* Douglas. Guolong section, TLK1c, PZ Aptian 4, sample 13GL142. 2, 4-5 *Mesorbitolina texana* (Roemer), 2, Azhang section, TLK1d, PZ Albian 1, sample 12LS55, 4-5, Guolong section, TLK1d, PZ Albian 1, sample 13GL78. 6 *Mesorbitolina subconcava* (Leymerie). Guolong section, TLK1f, PZ Albian 3, sample 13GL41. 7 *Conicorbitolina* sp. A. Guolong section, TLK1h, PZ Cenomanian 1, sample 13GL30. 8 *Palorbitolinoides orbiculata* Zhang. Guolong section, TLK1d, PZ Albian 1, sample 13GL61. 9 *Palorbitolinoides hedini* Cherchi & Schroeder, Guolong section, TLK1e, PZ Albian 2 sample 13GL56. In 1-4, 6-9, scale bars = 1 mm, 5, scale bar = 0.3 mm.

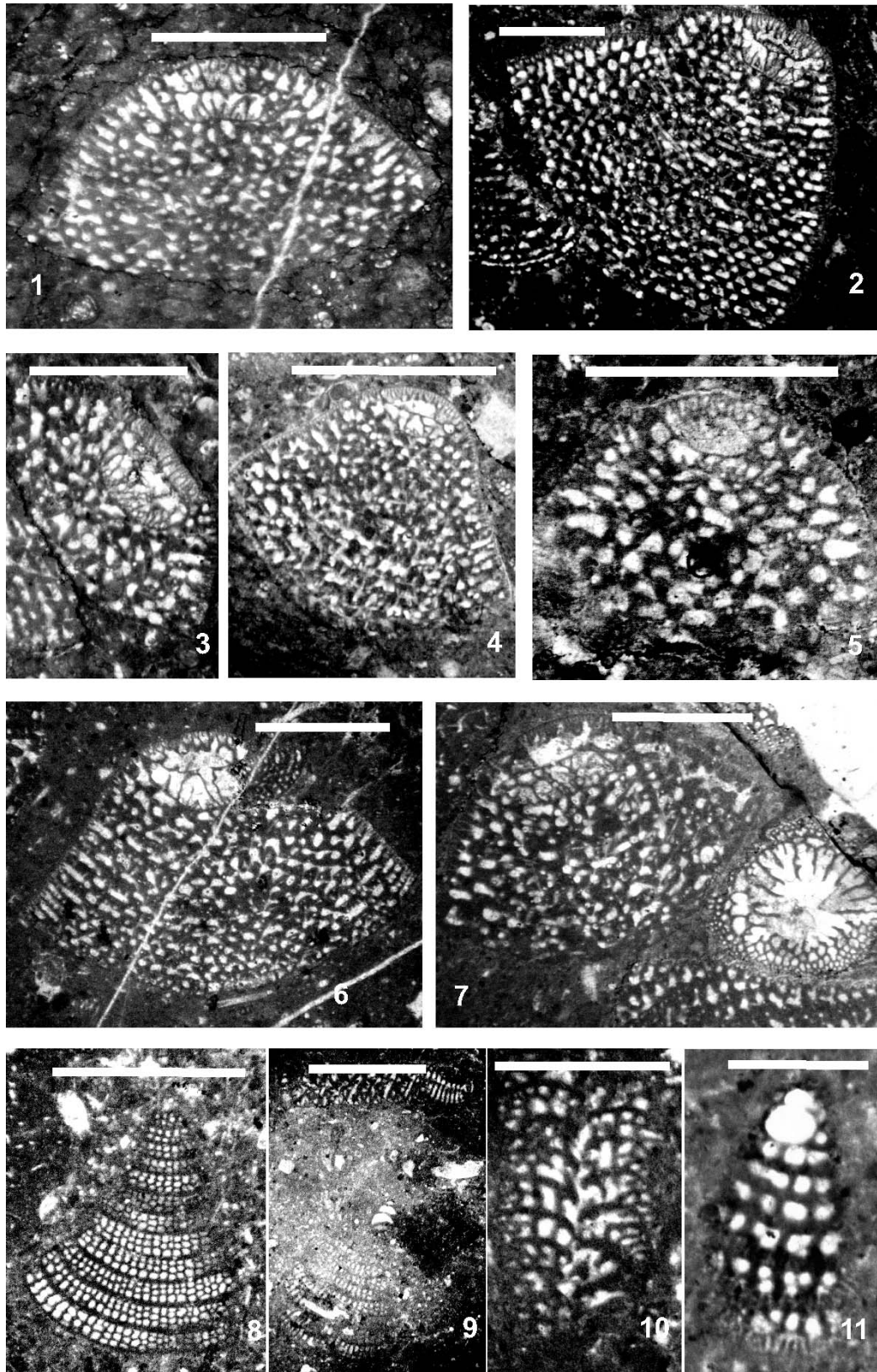


FIGURE 11. 1–4, 6–7. *Mesorbitolina aperta* (Erman), Guolong section, 1–3, TLK1f, PZ Albian 3, 1 sample 13GL46, 2–3, sample 13GL41, 4, TLK1h, PZ Cenomanian 1, 13GL30, 6, TLK1h, PZ Cenomanian 1, 7, oblique axial and oblique equatorial sections, sample 13GL30. 5 *Mesorbitolina subconcava*, Guolong section, TLK1d, PZ Albian 1, sample 13GL83. 8–10 *Cuneolina pavonia* d’Orbigny, Azhang section, 8, TLK1h, PZ Cenomanian 1, sample 12LS92, 9, TLK1d, PZ Albian 1, sample 12LS27, 10, TLK1d, PZ Albian 1, sample 12LS21. 11 *Vercorsella arenata* Arnaud-Vanneau. Guolong section, TLK1c, PZ Aptian 4, sample 13GL162. In 1–10, scale bars = 1 mm, 11, scale bar = 0.3 mm.

conch and subembryonic zone. Zhang (1982, 1986) described similar species to *M. subconcava* from the Lower Cretaceous of the Lhasa Block, Tibet (see above synonyms).

Distribution. This species is found in this study in the Aptian and Albian (latest Aptian 4a–Albian 4, upper part of TLK1c–TLK1g) of Azhang, Guolong sections and in the Coqen basin.

Mesorbitolina aperta (Erman, 1854)

Figs. 11.1–11.4, 11.6–11.7

Orbitolites apertus Erman, 1854, p. 603–60, pl. 23, figs. 1–3.

Orbitolina (Mesorbitolina) gigantea Zwang, 1986, p. 115, pl. 7, figs. 8–10.

Orbitolina (Orbitolina) toihaica Zwang, 1986, p. 116, pl. 8, figs. 8–11.

Discussion. This species is characterized by a deuteroconch subdivided in the upper part by several partitions of different sizes, whereas the lower part exhibits an irregular network of partitions. Zhang (1986) created two new species, *O. (M.) gigantea* and *O. (O.) toihaica*, that are similar to *M. aperta* from the lower Cretaceous of the Lhasa Block (Tibet).

Distribution. This species is found in this study in the Albian to Cenomanian (Albian 3–Cenomanian 1, upper part of TLK1g–TLK1h) of Azhang, Guolong sections and in the Coqen basin.

Genus: *Praeorbitolina* Schroeder, 1964

Type species: *Praeorbitolina cormyi* Schroeder, 1964

Praeorbitolina wienandsi Schroeder, 1964

Fig. 12.1

Praeorbitolina wienandsi Schroeder, 1964, p. 412, text-fig. B.

Orbitolina (Eorbitolina) robusta, Zhang, 1982, p. 74, pl. 1, figs. 10–13.

Discussion. *Praeorbitolina wienandsi* is distinguished in having an embryo followed by an initial spiral of only 2–3 cuneiform postembryonic chamber layers. It was described as *O. (E.) robusta* new species by Zhang, 1982 from the Aptian of Takena Formation in Xizang, China.

Distribution. This species is found in this study in the Aptian (PZ Aptian 2–late TLK1a) in Jiarong, Laxue, Azhang and Guolong sections and in the Linzhou basin.

PHYLOGENETIC EVOLUTION AND BIOZONATION

In our study, 16 species of orbitolinids forming four different lineages have been recognized (see Fig. 8). They belong to the *Palorbitolina lenticularis*–*Palorbitolinoides hedini* lineage (Cherchi & Schroeder, 2013); *Praeorbitolina cormyi*–*Mesorbitolina texana* lineage (Cherchi & Schroeder, 2013), which extends into the here newly identified *Mesorbitolina subconcava*–*Mesorbitolina birmanica*–*Mesorbitolina aperta* lineage; and the *Conicorbitolina* lineage. *Orbitolinopsis* has been here registered for the first time from Tibet from the Late Aptian of Tibet.

Cherchi & Schroeder (2013) traced the evolution of *Praeorbitolina cormyi* to *Mesorbitolina aperta* without integrating *M. birmanica* in the lineage. *Mesorbitolina birmanica* was first insufficiently described in 1937 by Sahni, however, the de-

scription of the types was subsequently emended by Sahni & Sastri (1957). *Mesorbitolina birmanica* has been identified by many authors from Tibet, Iran, and India (see Schlagintweit & Wilmsen, 2014; Rao et al., 2015). It is characterized by a bi-convex embryonic apparatus, which includes a plano-convex protoconch and a deuteroconch that is irregularly subdivided by occasional partitions. It is considered here as belonging to the ancestral stock of the *Mesorbitolina subconcava*–*aperta* group with a comparatively larger and more complex embryonic apparatus. The deuteroconch in *M. subconcava* is generally subdivided by short subdivision, which reach the lower part of the protoconch (Schroeder et al., 2010), while the deuteroconch of *M. aperta* is initially subdivided by several sets of alveoli, which become intense and irregular in the advanced forms in the Early Cenomanian. *Mesorbitolina birmanica* has been previously reported from Tibet by Zhang (1982, 1986, 1991), and ranges here from latest Aptian (Aptian 4b, 115.0 Ma) to Late Albian (Albian 4, 100.5Ma). On the other hand, *M. subconcava* ranges from Late Aptian (latest Aptian 4a, 116.0Ma) to Late Albian (Albian 4, 100.5Ma), while *M. aperta* is Late Albian (Albian 3, 106.7Ma) to Early Cenomanian in age (Cenomanian 1, 98.8 Ma).

Orbitolinopsis and *Paleodictyoconus* are common in the upper Aptian assemblages. We refer to them as *Orbitolinopsis* sp. A and *Paleodictyoconus* sp. A. on the basis of limited material. In this lineage, *Orbitolinopsis* sp. A occurs in the earliest Late Aptian (earliest Aptian 4). The test is relatively small, up to 1 mm in diameter, conical with a flat base. Its apex is twisted as in *Urgonina*, however the first coil is lost, leaving just an off-centered embryonic apparatus and the radial partitions anastomose centrally to form a reticulate zone in transverse section. The chambers are rectangular to discoidal, lacking tiers of peripheral chamberlets. The off-centered proloculus is globular, slightly larger than the oval deuteroconch. *Paleodictyoconus* sp. A occurs in the latest Late Aptian (latest Aptian 4), and is characterized by a narrow marginal zone that is subdivided by radial beams, with those of adjacent rows alternating in position. The off-centered proloculus is still globular, but is followed directly by a small deuteroconch and a small spire of peri-embryonic chambers. This species differs from the Early Cretaceous *Paleodictyoconus arabicus* (Henson) in having fewer concentrated partitions.

Conicorbitolina first appears in the Late Albian (Albian 4, 102.2 Ma) as *C. cf. cuvillieri*, a markedly conical species with a spherical embryonic apparatus, partially obscured in many sections. However, the spherical protoconch and the cup-shaped deuteroconch clearly defines this species as *Conicorbitolina*. The relatively small size of the embryonic apparatus (~0.2 mm in diameter), and the subembryonic area divided by many radial partitions are comparable with typical *C. cuvillieri*. *Conicorbitolina* develops a much larger embryon (0.8–0.9 mm) in the Cenomanian, and develops into a less conical form, described here as *Conicorbitolina* sp. A. Due to limited material, however, both forms are indeterminable at the specific level.

The co-occurrence of LBF with PF at some levels of the mid-Cretaceous is vital for the correlation and refining the biostratigraphy of some of the long-ranging LBF. All the LBF were identified and the main species are plotted in Figure 9, in relation to the proposed foraminiferal biozona-

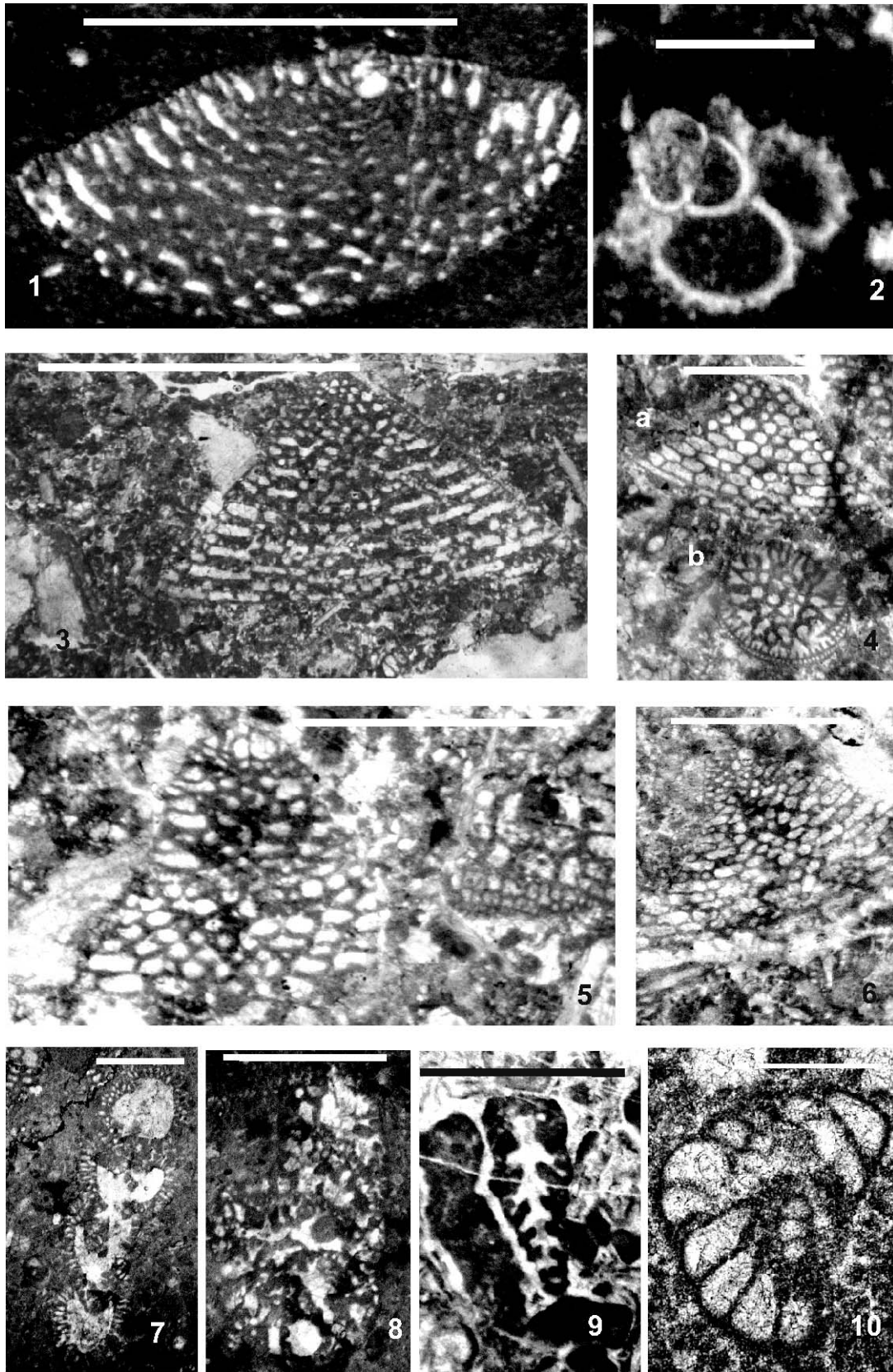


FIGURE 12. 1 *Praeorbitolina* cf. *wienandsi* Schroeder, Guolong section, TLK1g, PZ Albian 4, sample 13GL35. 2 *Favusella washitensis* (Carsey), Azhang section, TLK1e, PZ Albian 2, sample 12LS53. 3, 4b *Paleodictyoconus* sp. A. Guolong section, early TLK1c, early part of Aptian 4, sample 13GL187. 4a, 5–6. *Orbitolinopsis* sp. A. Guolong section, 4a, 5, TLK1c, PZ Aptian 4, sample 13GL187, 6, TLK1c, PZ Aptian 4, sample 13GL142. 7–8 *Pseudochoffatella cuvillieri* Deloffre, Guolong section, TLK1g, Albian 4, sample 13GL40. 9 *Everticyclammina* sp. A. Azhang section, TLK1c, Aptian 4, sample 12LS17. 11 *Nezzazata conica* (Smout), Azhang section, TLK1h, PZ Cenomanian 1, sample 12LS92. Scale bars = 1 mm, except for 2, 7–10, scale bar = 0.3 mm.

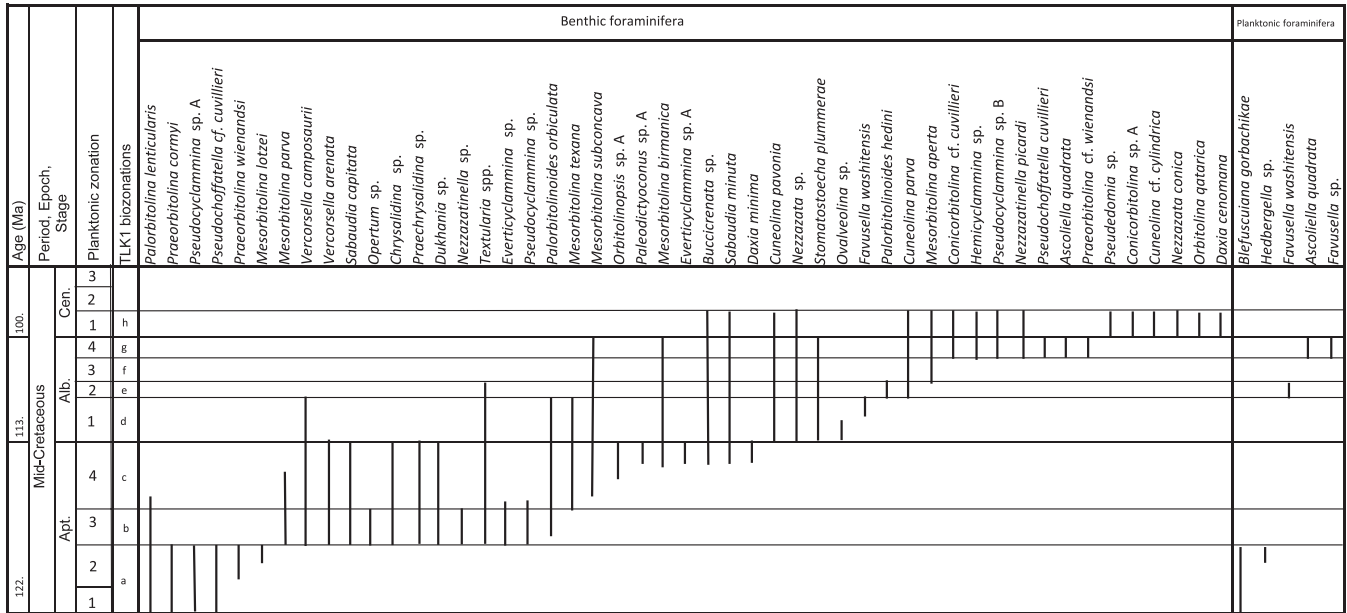


FIGURE 13. Range chart of key benthic and planktonic foraminiferal species of the Tibetan Platform. Planktonic Zones after BouDagher-Fadel (2013).

tions. In our definitions of stratigraphic ranges, we primarily use the PF zonal scheme of BouDagher-Fadel (2013), which is tied to the time scale of Gradstein et al. (2012). The integration of the material described in this study has enabled us to define eight mid-Cretaceous biozones that extend the previous Tibetan biozones for the Late Cretaceous and Early Paleocene described by BouDagher-Fadel et al. (2015):

- **TLK1a** (Jiarong section 13LZ18–13 and Laxue section 14LZ18–12 in the Linzhou basin, PZ Aptian 1–2, 126.3–119.5 Ma). This biozone is characterized by the first appearance of *Pseudochoffatella cf. cuvillieri* (Fig. 9.9). It includes primitive orbitolinids, such as *Palorbitolina lenticularis* (Fig. 9.1) and planispiral forms with alveolar walls, such as *Pseudocyclammina* sp. A (Fig. 9.8). *Praeorbitolina wienandsi* (Fig. 9.2a), *Praeorbitolina corymi* (Figs. 9.2b, 9.3–9.7) and *Mesorbitolina lotzei* made their first appearances in the upper part of this biozone.
- **TLK1b** (Azhang section in the Coqen basin: 12LS01–12LS05, PZ Aptian 3, 119.5–116.5 Ma). This biozone is characterized by the first appearance of *Mesorbitolina parva* (Figs. 10.1, 10.3). *Palorbitolina lenticularis*, *Palorbitolinoides orbiculata* with rare ataxophragmids, such as *Vercorsella camposaurii*, *V. arenata*, *Sabaudia capitata*, *Opertum* sp., triserial to biserial chrysalinids such as *Chrysalidina* sp., *Praechrysalidina* sp., *Dukhanina* sp., rare nezzazatids, such as *Nezzazatinella* sp., small miliolids, *Textularia* spp., agglutinated foraminifera with alveoles such as *Everticyclammina* sp. and *Pseudocyclammina* sp. A, as well as rare dasyclads, are also present.
- **TLK1c** (Azhang section 12LS06–17 and Guolong section 13GL195–141 in the Coqen basin, PZ Aptian 4, 116.5–113.0 Ma; Sangzugang section 10SZG–B, C, 04, 10 in the Xigaze basin). This biozone is characterized by the first appearance of *Mesorbitolina texana* (Figs. 10.2, 10.4–10.5).

Mesorbitolina parva (Figs. 10.1, 10.3), *M. birmanica* (Fig. 9.10), *Palorbitolinoides orbiculata*, *Sabaudia capitata*, *Vercorsella camposaurii*, *V. arenata*, (Fig. 11.11) *Orbitolinopsis* sp. A (Figs. 12.4a–12.6), *Paleodictyoconus* sp. A. (Figs. 12.3–12.4b) are common. *Palorbitolina lenticularis* become extinct within the early part of this biozone where assemblages are dominated by robust, shallow, clear-water, convex to concave forms of orbitolinids. In the upper part of this biozone, orbitolinids are replaced gradually by small agglutinated forms, such *Everticyclammina* sp. A (Fig. 12.9), *Pseudocyclammina* spp., *Buccicrenata* spp., *Chrysalidina* sp., *Vercorsella arenata*, *Mayncina* sp., *Daxia minima*, *Sabaudia minuta*, *S. capitata*. Rare *Mesorbitolina texana* remain constantly present with rare species of *M. subconca* appearing for the first time. Codiacean, dasyclad algae and gastropod spp. are common. *Everticyclammina* sp. A (Fig. 12.9), planispiral with a very short initial coil, followed by an elongate uniserial part with a single areal aperture and an alveolar wall with the septa remaining solid, dominate the assemblages. This species is similar to the advanced *E. greigi* (see BouDagher-Fadel, 2008) in which the lower parts of the adult septa are oblique, then tangential to the spiral suture, and thicken and coalesce to form imperforate basal layers to the chambers.

- **TLK1d** (Azhang section 12LS18–56, Guolong section 13GL86–59 and 13GL196 in the Coqen basin, PZ Albian 1, 113.0–109.8 Ma). This biozone is characterized by the first appearance of *Cuneolina pavonia* (Fig. 11.8) and *Nezzazata* sp. Assemblages include *Mesorbitolina texana*, *M. subconca*, *M. birmanica*, *Palorbitolinoides orbiculata* (Fig. 10.8), *Buccicrenata* sp., *Stomatostoecha plummerae*, *Nezzazata* sp., *Nezzazatinella* sp., *Cuneolina parva*, *Sabaudia minuta*, *Vercorsella scarsellai*, *Pseudocyclammina* sp., and *Ovalveolina* sp. Small miliolids and dasyclad algae are common.

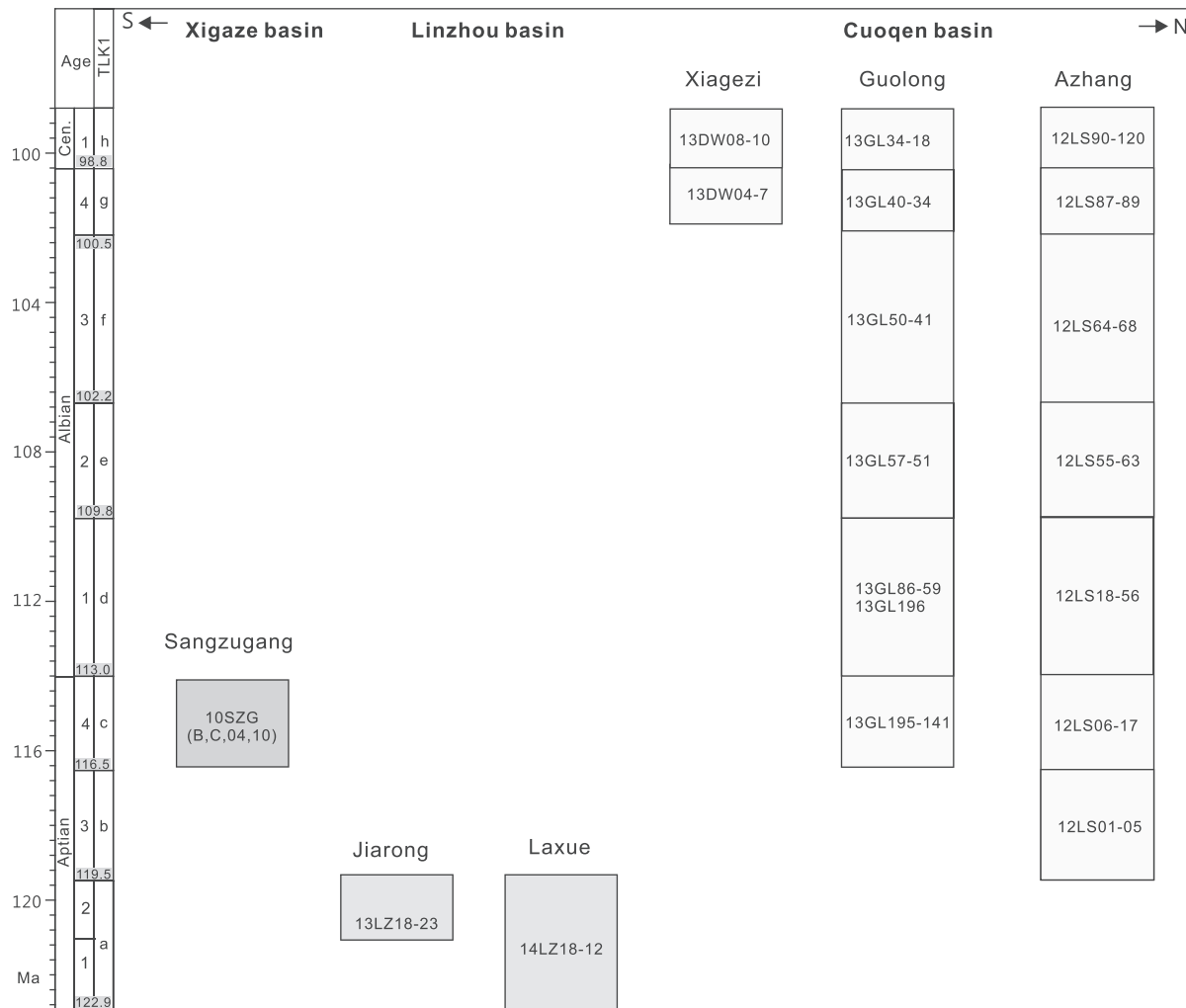


FIGURE 14. Age and LBF biozone distribution of mid-Cretaceous limestones from the Xigaze basin, the Linzhou basin and the Coqen basin in the Lhasa terrane. Sample numbers correspond to those in Figures 2–6.

- **TLK1e** (Azhang section 12LS55–63 and Guolong section 13GL57–51 in the Coqen basin, PZ Albian 2, 109.8–106.7 Ma). This biozone is characterized by the first appearance of *Palorbitoloides hedini* (Fig. 10.9). Assemblages include *Mesorbitolina subconca* (Figs. 10.6, 11.5), *M. birmanica*, *Palorbitoloides orbiculata*, *Vercorsella scarsellai*, *Buccicrenata* sp., *Sabaudia minuta*, *Cuneolina parva*, *C. pavonia* and small miliolids. Planktonic foraminifera such as *Favusella washitensis* (Fig. 12.2) and dasyclad algae are also rare.
- **TLK1f** (Azhang section 12LS64–86 and Guolong section 13GL50–41 in the Coqen basin, PZ Albian 3, 106.7–102.2 Ma). This biozone is characterized by the first appearance of *Mesorbitolina aperta* (Figs. 11.1–11.4, 11.6–11.7). Assemblages are dominated by *Mesorbitolina subconca*, *M. birmanica*, *Vercorsella scarsellai*, *Buccicrenata* sp., *Cuneolina pavonia* and *Textularia* spp.
- **TLK1g** (Azhang section 12LS87–89, Guolong section 13GL40–34 and the Xiagezi section 13DW04–7 in the Coqen basin, PZ Albian 4, 102.2–100.5 Ma). This biozone is characterized by the first appearance of *Pseudo-*

choffatella cuvillieri (Figs. 12.7–12.8). Assemblages include *Mesorbitolina subconca*, *M. aperta*, *M. birmanica*, *Cuneolina pavonia*, *Vercorsella scarsellai*, *Sabaudia minuta*, *Buccicrenata* sp., *Hemicyclammina* sp., *Pseudocyclammina* cf. *rugosa*, *Pseudocyclammina* sp. B, *Conicorbitolina* cf. *cuvillieri*, *Stomatostoecha plummerae*, *Nezzazata* sp., *Nezzazatinella picardi*, and rare planktonic foraminifera *Ascoliella quadrata*, *Favusella* sp. are also present. We have also found in this assemblage a primitive form, *Praeorbitolina* cf. *wienandsi* (Fig. 12.1), thus extending the range of *Praeorbitolina* to the top of the Albian in this area.

- **TLK1h** (Azhang section 12LS90–120, Guolong section 13GL34–18, Xiagezi section 13DW07–11 in the Coqen basin, PZ Cenomanian 1, 100.5–98.8 Ma). This biozone is characterized by the first appearance of *Conicorbitolina* sp. A (Fig. 10.7) and *Nezzazata conica* (Fig. 12.11). Assemblages include *Mesorbitolina aperta* (Figs. 11.1–11.4, 11.6–11.7), *Conicorbitolina* cf. *cuvillieri*, *Sabaudia minuta*, *Cuneolina* cf. *cylindrica*, *Pseudocyclammina* sp. B, *Cuneolina parva*, *C. pavonia* (Fig. 11.8–11.10), *Daxia cenomana*, *Nez-*

zazatinella picardi, *Buccicrenata* sp., *Pseudocyclammina* sp. B and *Pseudedomia* sp.

The almost continuous sedimentary sequences also allowed the recognition of four phylogenetic lineages for the Tibetan orbitolinids, namely:

- the *Praeorbitolina*–*Mesorbitolina* lineage of Aptian – Early Cenomanian age, previously defined by Cherchi & Schroeder (2013) is confirmed. However, we also prove the range of the Early Aptian *Praeorbitolina* of this lineage extends to the top of the Albian in the Tibetan platform (Fig. 12.1, 13), and we integrate *Mesorbitolina birmanica*, which exhibit a rather large and complex biconvex embryonic apparatus with a plano-convex protoconch, within the Early Aptian to Early Cenomanian *Mesorbitolina* lineage (*M. lotzei*–*M. aperta*);
- the *Palorbitolina*–*Palorbitolinoides* lineage of Aptian–Albian age, previously defined by Cherchi & Schroeder (2013) is also confirmed. However, we extend the range of *Palorbitolina lenticularis* into the latest Late Aptian. In addition, we prove that the age of *Palorbitolinoides orbiculata* extends into the Early Albian (see Fig. 13 for age range of key species).

Our data show that the Takena limestones in the Linzhou basin have an Aptian 1, TLK1a, age while the Sangzugang limestones in the Xigaze basin correspond to the age of Aptian 4, TLK1c. The Langshan limestones have a relatively longer duration spanning from Aptian 3, TLK1b to Cenomanian 1, TLK1h. The age and LBF biozone correlation of mid-Cretaceous limestones in the three sedimentary basins of the Lhasa terrane are shown in Figure 14.

PALEOENVIRONMENTS OF THE MID-CRETACEOUS CARBONATE FACIES

The mid-Cretaceous was a globally warm period, characterized by an increase in the number of agglutinated foraminiferal forms having large alveoles, such as *Pseudocyclammina*, or forms with internal radial partitions, such as the orbitolinids. This may have been an adaptation to the extreme climatic and oceanic conditions (increases in temperature and oceanic anoxia; e.g., Kerr, 2006) during this interval (BouDagher-Fadel, 2008), linked to an inferred dramatic increase of carbon dioxide in the atmosphere possibly triggered by enhanced global volcanism (e.g., the Ontong Java flood events). The high CO₂ levels during this greenhouse period also would have led to increased oceanic acidity (Naafs et al., 2016), which would have favored the development and ecological domination of agglutinated LBF forms, such as the orbitolinids, over those forms with biogenically precipitated calcitic tests that dominated before and after this period.

As seen above, the mid-Cretaceous shallow-marine limestones, which today occur in the Tibetan Plateau, have fossil assemblages that are dominated by the agglutinated orbitolinids, although *Pseudocyclammina* and *Dictyoconus* are also present. These agglutinated LBF thrived in many shallow carbonate environments (Arnaud Vanneau, 1980). The conical tests of the orbitolinids were strengthened by subdividing it into many small chamberlets, which likely housed

within their walls symbiotic algae (see BouDagher-Fadel, 2008). By studying the size and shape of their tests, Masse (1976) deduced that they had a free, epifaunal mode of life. They lived on the sea-floor substrate, on the flat base of their conical test. Using associated algae, Banner & Simmons (1994) noted that *Palorbitolina lenticularis* was most common in sediments thought to be deposited at depths of 10–50 m. Orbitolinid-rich beds, with large, flat, orbitolinids seem to be characteristic of transgressive deposits, while more conical forms thrived in the shallowest water (Vilas et al., 1995; Simmons et al., 2000). This relationship of shape to palaeobathymetry has been observed in different studies on living larger foraminifera; for example, Reiss & Hottinger (1984) observed a flattening of *Operculina* tests with increasing water depth.

During this time, adaptive radiations in test shape and environmental control of growth-forms make LBF reliable paleoenvironmental indicators (see Simmons et al., 2010). Sedentary, attached LBF grew to accommodate the shape of the phytal substrate to which they adhered (BouDagher-Fadel & Wilson, 2000). Those found attached on sediments in deeper waters tend to be flat and discoidal in shape (see BouDagher-Fadel, 2008). However, LBF are also very sensitive to light levels (BouDagher-Fadel, 2008), and water clarity is an important factor in their distribution and the way they grow. Being unicellular, LBF exhibit relatively rapid adaptation to environmental conditions through evolutionary modifications of their shape and structure. For example, shallow-water settings with high clay content have populations of larger orbitolinids similar to those of the deeper water environments (Pittet et al., 2002). It is therefore, essential to analyse not only the shape of the orbitolinids, but all associated foraminifera and sediments to deduce their paleoenvironment. On this basis therefore, we can combine the analysis of the shape of the orbitolinids with that of the associated microfaunas and microfloras to infer the palaeoenvironmental history of the margin of the East Tethyan ocean during the mid-Cretaceous as follows (see Fig. 15):

- A regressive phase of shallow reefal environments where small primitive orbitolinids, such as *Praeorbitolina* spp., dominated (TLK1a).
- A transgressive phase (TLK1b) of reefal to foreereefal environments with assemblages dominated by large, flat-shaped orbitolinids (flattest around the maximum flooding surface).
- A reefal environment (TLK1c) shallowing abruptly to a backreef setting where orbitolinids are replaced by *Everticyclammina* spp. and small conical ataxophragmids (e.g. *Vercorsella arenata*). These two phases of sea-level change were identified by Miller et al. (2011; see Fig. 7).
- A transgressive phase (TLK1d) with the flat forms of *Mesorbitolina texana* dominating the assemblages. Many of the specimens of *M. texana* in the Guolong section were well-sorted in size and direction by wave action, reflecting their deposition in a high energy foreereef environment (see Fig. 15).
- A regressive phase (TLK1e) where assemblages were dominated by small, broadly conical forms of orbitolin-

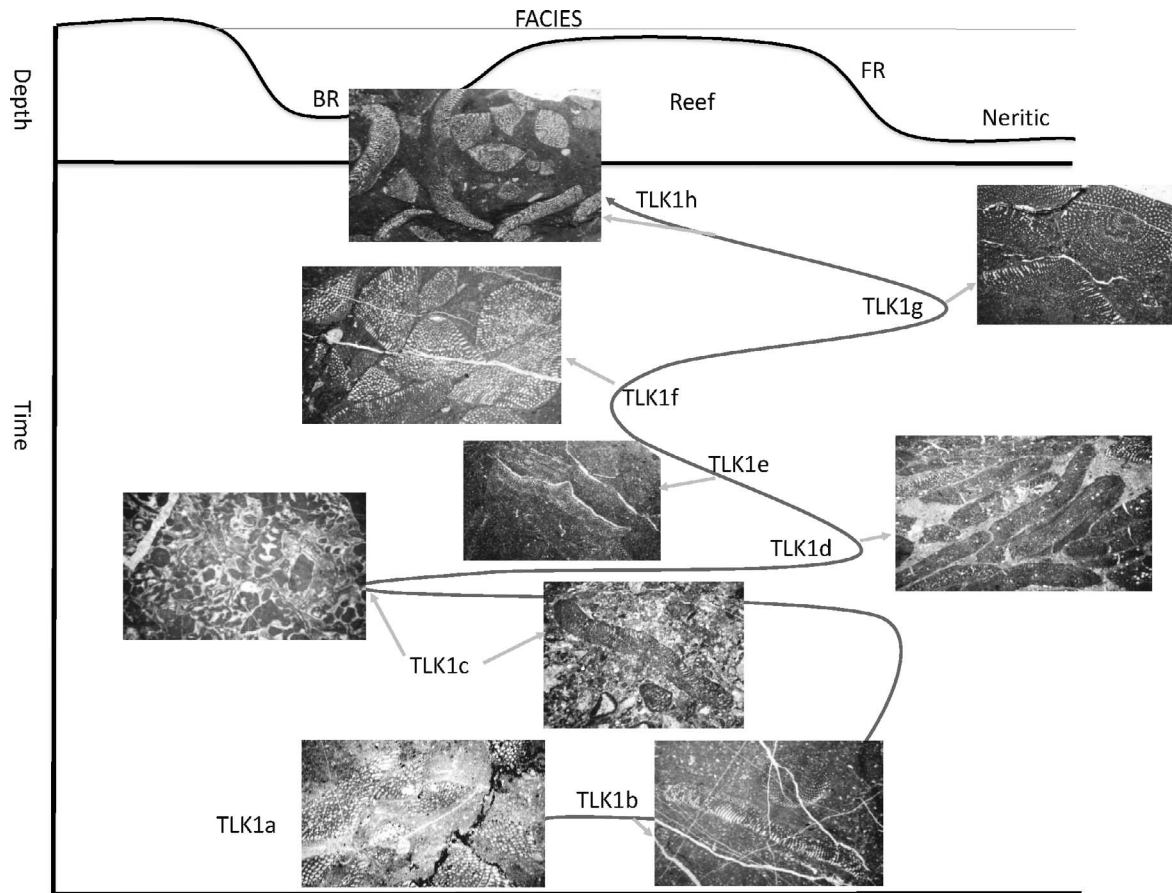


FIGURE 15. The depositional environments that prevailed during the mid-Cretaceous on the Tibetan Platform; global sea-level variation after Miller et al. (2011).

ids (e.g., *Palorbitolinoides hedini*, Fig. 10.9). Planktonic foraminifera were present, but rare (e.g., *Favusella washitensis*, Fig. 12.2) indicating a low energy, open-marine reefal environment.

- A regressive phase (TLK1f) where assemblages were dominated by broadly conical (e.g., *Mesorbitolina subconca*, Figs. 10.6, 11.5) to small convex orbitolinids (e.g., *Mesorbitolina aperta*, Figs. 11.1–11.4, 11.6–11.7) with abundant fragments of rhodophyte and dasyclad algae indicating a shallow reefal environment.
- A transgressive phase (TLK1g) of a reefal to forereef environment, reflecting the reported (Miller et al., 2011) rapid sea-level rise of over 50 m (see Fig. 7). Assemblages were dominated by broadly convex and flat orbitolinids (see Fig. 15). Planktonic foraminifera and forms with coarsely agglutinated epidermis, such as *Pseudochoffatella cuvillieri* (Figs. 12.7–12.8) were also frequent.
- A regressive phase (TLK1h) where foraminiferal assemblages were dominated by conical, relatively small orbitolinids, but with complicated embryonic apparatus (e.g., *Mesorbitolina aperta*, see Figs. 11.1–11.4, 11.6–11.7), and small ataxophragmids, indicating the re-establishment of shallow reefal conditions following the reported (Miller et al., 2011) 50 m sea regression in the Early Cenomanian (see Fig. 7).

COMPARISON WITH THE LBF IN WESTERN TETHYS

We found that the mid-Cretaceous carbonate successions in the Tibetan Himalayas evolved through eight depositional stages (see Fig. 15), which correlate well with the global sea level curve for this interval (Miller et al., 2011; see Fig. 7), and from which we created eight biozones (TLK1a–h). The occasional presence of PF with orbitolinids (e.g., Fig. 12.2) provided the opportunity to define the biostratigraphic framework of the LBF in the studied sections. The biozones created in this study for the mid-Cretaceous of the Tibetan platform enables the correlation between the Langshan, Sangzugang and Takena Formations in the Lhasa terrane.

A comparison between the mid-Cretaceous LBF associations of the Tibetan carbonate platforms with those of the southern Neo-Tethys margin and of southwest Europe show that the LBF are comparable with those developed over large parts of the Tethyan realm. The Tibetan orbitolinids seem to have only very few latest Aptian–Albian species (*Palorbitolina lenticularis*, *Mesorbitolina texana*, *M. parva*) in common with those of North America, however, Albian and Early Cenomanian lineages are comparable with those of Europe and the eastern Arabian Plate (see Schroeder, 2010). We further confirmed the *Praeorbitolina cormyi*–*Mesorbitolina*

texana and the *Palorbitolina lenticularis*–*Palorbitolinoides hedini* lineages of Cherchi & Schroeder (2013), but also integrated a new *Mesorbitolina birmanica*–*Mesorbitolina aperta* lineage. Finally, we were also able to extend the range of the Early Aptian *Praeorbitolina* (e.g., *Praeorbitolina cf. wienandsi*, Fig. 12.1) to the top of the Albian, and present a revised range chart of the Tibetan forms in Fig. 13.

CONCLUSION

The foraminiferal-bearing facies, used here as biostratigraphic and paleoenvironmental indicators, enabled us to define eight new biozones (TLK1a–h), which complement the Late Cretaceous and Neogene biozones for this region previously described by BouDagher-Fadel et al. (2015). The biozonations erected here are based on the stratigraphic first occurrences of index foraminifera. The limestones are rich in LBF, the most significant of which are orbitolinids as they have long been recognized as useful biostratigraphic markers in mid-Cretaceous Tethyan carbonate platforms (Henson, 1948; Douglass, 1960; Schroeder, 1962, 1975; Hofker, 1963; Neumann, 1967; Arnaud Vanneau, 1975, 1980; Cherchi & Schroeder, 1980, 2013; Marcoux et al., 1987; Görög & Arnaud Vanneau, 1996). Occasionally, the deeper water LBF assemblages co-occur or are interspersed with PF assemblages. The well-established PF biostratigraphic ranges (see BouDagher-Fadel, 2013, 2015) have enabled the confirmation and delineation of the biostratigraphic ranges of these co-existing LBF.

In addition to enabling the development and refinement of the eastern Tethyan carbonate biostratigraphy, these assemblages allowed inference of details of the paleoenvironment: the paleoenvironment was interpreted from the changes in the foraminiferal facies throughout the sedimentary succession. In the backreef carbonate facies, ataxophragmiids and everticyclamminids dominated the foraminiferal assemblages of small miliolids and textularids. However, in the reefal to outer neritic environments, orbitolinid facies dominated. The inferred paleoenvironmental development of the region correlates very well with the global sea-level variation deduced by Miller et al. (2011)

ACKNOWLEDGMENTS

We thank Zhong Han and Wei Zhang for their assistance in sampling the field. This study was financially supported by the Most 973 Project (2012CB822001) and the NSFC Project (41472081). We would also like to thank Mike Simmons for discussion on some species of *Orbitolina*.

REFERENCES

- An, W., Hu, X., Garzanti, E., BouDagher-Fadel, M. K., Wang, J., and Sun, G., 2014, Xigaze forearc basin revisited (South Tibet): Provenance changes and origin of the Xigaze Ophiolite: Geological Society of America Bulletin, v. 126, p. 1595–1613.
- Arnaud Vanneau, A., 1975, Réflexion sur le mode de vie de certains Orbitolinidés (Foraminifères) barrémo-aptiens de l'Urgonien du Vercors: Compte rendu des séances de la société de physique et d'histoire naturelle de Genève, v. 10 fascicule, p. 126–130.
- Arnaud Vanneau, A., 1980, Micropaléontologie, paléocologie et sédimentologie d'une pl.-forme carbonatée de la marge passive de la Téthys: l'Urgonien du Vercors septentrional et de la Chartreuse (Alpes occidentales): Géologie Alpine, v. 11, p. 1–874.
- Banner, F. T., and Simmons, M. D., 1994, Calcareous algae and foraminifera as water-depth indicators: an example from the Early Cretaceous carbonates of Northwest Arabia, in Simmons, M. D. (ed.), Micropalaeontology and Hydrocarbon Exploration in the Middle East: Chapman and Hall, London, p. 243–252.
- Bassoullet, J. P., Colchen, M., Mascle, G., and Wang, N., 1984, Les ensembles sédimentaires de la zone du Tsangpo (Lhaze, Lhasa, Linzhu), in Mercier, J. L., Li, Guangcen (eds.), Mission Franco-Chinoise au Tibet, 1980: Centre National de la Recherche Scientifique, Paris, p. 133–153.
- BouDagher-Fadel, M. K., 2008, Evolution and Geological Significance of Larger Benthic Foraminifera, Developments in Palaeontology and Stratigraphy: Elsevier, Amsterdam, v. 21, 540 p.
- BouDagher-Fadel, M. K., 2013, Diagnostic First and Last Occurrences of Mesozoic and Cenozoic Planktonic Foraminifera: Professional Papers Series, 1, OVPRL UCL, London, p. 1–4.
- BouDagher-Fadel, M. K., 2015, Biostratigraphic and Geological Significance of Planktonic Foraminifera (Updated 2nd Edition): UCL Press, London, . doi:10.14324/111.9781910634257.
- BouDagher-Fadel, M. K., and Wilson, M., 2000, A revision of some larger foraminifera of the Miocene of southeastern Kalimantan: Micropaleontology, v. 46, p. 153–165.
- BouDagher-Fadel, M. K., Price, G. D., Hu, X., and Li, J., 2015, Late Cretaceous to early Paleogene foraminiferal biozones in the Tibetan Himalayas, and a pan-Tethyan foraminiferal correlation scheme: Stratigraphy, v. 12, p. 67–91.
- Cherchi, A., and Schroeder, R., 1980, *Palorbitolinoides hedini* n. gen. n. sp., grand foraminifère du Crétacé inférieur du Tibet meridional: Comptes rendus de l'Académie des Sciences Paris, Series D 291, p. 385–388.
- Cherchi, A., and Schroeder, R., 2013, The *Praeorbitolina/Palorbitolinoides* Association: an Aptian biostratigraphic key-interval at the southern margin of the Neo-Tethys: Cretaceous Research, v. 38, p. 70–77.
- Chu, M. F., Chung, S. L., Song, B. A., Liu, D. Y., O'Reilly, S. Y., Pearson, N. J., Ji, J. Q., and Wen, D. J., 2006, Zircon U-Pb and Hf isotope constraints on the Mesozoic tectonics and crustal evolution of Southern Tibet: Geology, v. 34, p. 745–748.
- Douglass, R. C., 1960, The Foraminiferal Genus *Orbitolina* in North America: Geological Survey Professional Paper, v. 333, p. 1–52.
- Dürr, S. B., 1996, Provenance of Xigaze forearc clastic rocks (Cretaceous, south Tibet): Geological Society of America Bulletin, v. 108, p. 669–691.
- Erman, A., 1854, Einige Beobachtungen über die Kreideformation an der Nordküste von Spanien. Zeitschrift der Deutschen Geologischen Gesellschaft, v. 6, p. 596–611.
- Görög, A., and Arnaud Vanneau, A., 1996, Lower Cretaceous Orbitolinids from Venezuela: Micropaleontology, v. 42, p. 65–78.
- Gradstein, F. M., Ogg, J. G., Schmitz, M. D., and Ogg, G. M., 2012, The Geologic Time Scale 2012: Elsevier, Amsterdam, 1144 p.
- Harris, N. B. W., Inger, S., and Xu, R., 1990, Cretaceous plutonism in Central Tibet: An example of post-collision magmatism?: Journal of Volcanology and Geothermal Research, v. 44, p. 21–32.
- Henson, F. R. S., 1948, Larger Imperforate Foraminifera of South-Western Asia (Families Lituolidae, Orbitolinidae and Meandropsinidae): Xi, British Museum (Natural History), London, 127 p.
- Hofker, J., 1963, Studies on the genus *Orbitolina* (Foraminiferida): Leidse Geologische Medelingen, v. 29, p. 181–253.
- Hottinger, L., 1978, Comparative anatomy of elementary shell structures in selected larger Foraminifera, in Hedley, R. H., and Adams, C. G. (eds.), Foraminifera 3: Academic Press, London, p. 203–266.
- Ji, W. Q., Wu, F. Y., Chung, S. L., Li, J. X., and Liu, C. Z., 2009, Zircon U-Pb geochronology and Hf isotopic constraints on petrogenesis of the Gangdese Batholith, Southern Tibet: Chemical Geology, v. 262, p. 229–245.
- Kapp, P., Decelles, P. G., Gehrels, G. E., Heizler, M. and Ding, L., 2007, Geological records of the Lhasa-Qiangtang and Indo-Asian collisions in the Nima area of Central Tibet: Geological Society of America Bulletin, v. 119, p. 917–932.

- Kapp, P., Yin, A., Harrison, T. M., and Ding, L., 2005, Cretaceous-Tertiary shortening, basin development, and volcanism in central Tibet: Geological Society of America Bulletin, v. 117, p. 865–878.
- Kerr, R. A., 2006, Creatures great and small are stirring the ocean: Science, v. 313, p. 1717.
- Leeder, M. R., Smith, A. B., and Jixiang, Y., 1988, Sedimentology and palaeoenvironmental evolution of the 1985 Lhasa to Golmud Geotraverse: Philosophical Transactions of the Royal Society of London, series A 327, p. 107–143.
- Leier, A. L., Decelles, P. G., Kapp, P., and Ding, L., 2007, The Takena Formation of the Lhasa terrane, southern Tibet: The record of a Late Cretaceous retroarc foreland basin: Geological Society of America Bulletin, v. 119, p. 31–48.
- Leymerie, A., 1878, Description géologique et paléontologique des Pyrénées de la Haute-Garonne; Atlas: É. Privat, Toulouse, 2 v., 1010 p.
- Liu, C., Yin, J., Sun, X., and Sun, Y., 1988, Marine Late Cretaceous–Early Tertiary sequences: The non-flysch deposits of the Xigaze forearc basin in south Xizang: Journal of the Institute of Geology, China Academy of Science, v. 3, p. 130–157 (in Chinese).
- Marcoux, J., Girardeau, J., Fourcade, E., Bassoulet, J. E. P., Philip, J. M., Jaffrezo, M., Xuchang, X., and Chengfa, C., 1987, Geology and biostratigraphy of the Jurassic and lower Cretaceous series to the north of the Lhasa Block (Tibet, China): Geodinamica Acta (Paris), v. 1, p. 313–325.
- Masse, J.-P., 1976, Les calcaires urgoniens de Provence (Valanginian-Aptien), Stratigraphie, paléontologie, les paléoenvironnements et leur evolution: Thèse Doctorat D'Etat, Université Aix-Marseille, France, v. I, II, 445 p.
- Miller, K. G., Mountain, G. S., Wright, J. D., and Browning, J. V., 2011, A 180-million-year record of sea-level and ice volume variations from continental margin and deep-sea isotopic records: Oceanography, v. 24, p. 40–53.
- Naafs, B. D. A., Castro, J. M., De Gea, G. A., Quijano, M. L., Schmidt, D. N., and Pancost, R. D., 2016, Gradual and sustained carbon dioxide release during Aptian Oceanic Anoxic Event 1a: Nature Geoscience, v. 9, p. 135–139.
- Neumann, M., 1967, Manuel de Micropaléontologie des Foraminifères (Systématique - Stratigraphie): Gauthiers-Villars, Paris, 297 p.
- Pan, G. T., Ding, J., Yao, D. S., and Wang, L. Q., 2004, Guidebook of 1:1500000 Geologic Map of the Qinghai-Xizang (Tibet) Plateau and Adjacent Areas: China: Chengdu Cartographic Publishing House, Chengdu, p. 1–48 (in Chinese).
- Pearce, J. A., and Mei, H., 1988, Volcanic rocks of the 1985 Tibet Geotraverse: Lhasa to Golmud: Philosophical Transactions of the Royal Society of London, Series A 327, p. 169–201.
- Pittet, B., Van Buchem, F. S. P., Hillgärtner, H., Razin, P., Grötsch, J., and Droste, H., 2002, Ecological succession, palaeoenvironmental change, and depositional sequences of Barremian-Aptian shallow-water carbonates in northern Oman: Sedimentology, v. 49, p. 555–581.
- Rao, X., Skelton, P. W., Sha, J., Cai, H., and Iba, Y., 2015, Mid-Cretaceous rudists (Bivalvia: Hippuritida) from the Langshan Formation, Lhasa block, Tibet: Papers in Palaeontology, v. 1, p. 401–424.
- Reiss, Z., and Hottinger, L., 1984, The Gulf of Aqaba: Ecological Micropaleontology: Ecological Studies, v. 50, p. 1–354.
- Roemer, F., 1849, Texas: Mit besonderer Rücksicht auf deutsche Auswanderung und die physischen Verhältnisse des Landes nach eigener Beobachtung geschildert. pp. 1–464.
- Roemer, C. F., 1852, Die Kreidebildungen von Texas und organischen Einschlüsse: A. Marcus, Bonn, 100 p., 11 pl.
- Sahni, M. R., 1937, Discovery of *Orbitolina*-bearing Rocks in Burma; with a description of *Orbitolina birmanica* sp. nov: Records of the Geological Survey of India, v. 71, p. 360–375.
- Sahni, M. R., and Sastri, V., 1957, A monograph of the orbitolines found in the Indian continent (Chitral, Gilgit, Kashmir), Tibet and Burma, with observations on the age of the associated volcanic series: Palaeontologia Indica, v. 33, p. 1–44.
- Schlagintweit, F., and Wilmsen, M., 2014, Orbitolinid biostratigraphy of the top Taft Formation (Lower Cretaceous of the Yazd Block, Central Iran): Cretaceous Research, v. 4, p. 125–133.
- Schroeder, R., 1962, Orbitolinen des Cenomans Süd-westeuropas: Paläontologische Zeitschrift, v. 36, p. 171–202.
- Schroeder, R., 1964, Orbitoliniden-Biostratigraphie des Urgons nordostlich von Teruel (Spanien): Neues Jahrbuch für Geologie und Paläontologie, Monatshefte, p. 462–474.
- Schroeder, R., 1975, General evolutionary trends in orbitolinas: Revista española de Micropaleontología, Numero especial, p. 117–128.
- Schroeder, R., Van Buchem, F. S. P., Cherchi, A., Baghbani, D., Vincent, B., Immenhauser, A., and Granier, B., 2010, Revised orbitolinid biostratigraphic zonation for the Barremian – Aptian of the eastern Arabian Plate and implications for regional stratigraphic correlations: GeoArabia Special Publication 4, v. 1, p. 49–96.
- Scott, R., Wan, X., Sha, J., and Wen, S., 2010, Rudists of Tibet and the Tarim basin, China: significance to requeniidae phylogeny: Journal of Paleontology, v. 84, p. 444–465.
- Simmons, M. D., Whittaker, J. E., and Jones, R. W., 2000, Orbitolinids from Cretaceous sediments of the Middle East—a revision of the F.R.S. Henson and associated collection, in Hart, M. B., and Smart, C. W. (eds), Proceedings of the Fifth International Workshop on Agglutinated Foraminifera: Gybrowski Foundation Special Publication, v. 7, p. 411–437.
- Smith, A. B., and Xu, J., 1988, Palaeontology of the 1985 Tibet Geotraverse, Lhasa to Golmud: Philosophical Transactions of the Royal Society of London, ser. A, Mathematical and Physical Sciences, v. 327, p. 53–105.
- Sun, G., Hu, X., Sinclair, H. D., BouDagher-Fadel, M. K., and Wang, J., 2015, Late Cretaceous evolution of the Coqen Basin (Lhasa terrane) and implications for early topographic growth on the Tibetan Plateau: Geological Society of America Bulletin, v. 127, p. 1001–1020.
- Vilas, L., Masse, J.-P., and Arias, C., 1995, *Orbitolina* episodes in carbonate platform evolution, the early Aptian model from SE Spain: Palaeogeography Palaeoclimatology Palaeoecology, v. 119, p. 35–45.
- Wang, C., and Liu, Z., 1999, Xigaze forearc basin and Yarlung Zangbo suture zone, Tibet: Geological Publishing House (in Chinese), Beijing, 237 p.
- Wang, C., Li, X., Liu, Z., Li, Y., Jansa, L., Dai, J., and Wei, Y., 2012, Revision of the Cretaceous-Paleogene stratigraphic framework, facies architecture and provenance of the Xigaze forearc basin along the Yarlung Zangbo suture zone: Gondwana Research, v. 22, p. 415–433.
- Wang, J., Hu, X., Garzanti, E., and Wu, F., 2013, Upper Oligocene–Lower Miocene Gangrinboche Conglomerate in the Xigaze Area, Southern Tibet: Implications for Himalayan Uplift and Paleoyarlung-Zangbo Initiation: The Journal of Geology, v. 121, p. 425–444.
- XZBGM (Xizang Bureau of Geology and Mineral Resources), 1993, Regional geology of Xizang Autonomous Region, China, with geologic map, scale 1:1,500,000: Beijing, Geological Publishing House, 707 p.
- Yin, A., and Harrison, T. M., 2000, Geologic evolution of the Himalayan-Tibetan orogen: Annual Review of Earth and Planetary Sciences, v. 28, p. 211–280.
- Yin, J., Xu, J., Chengjie, L., and Huan, L., 1988, The Tibetan Plateau: Regional stratigraphic context and previous work: Philosophical Transactions of the Royal Society of London, ser. A, Mathematical and Physical Sciences, v. 327, p. 5–52.
- Zhang, B., 1982, *Orbitolina* (foraminifera) from Xisang. Series of the Scientific Expedition to the Qinghai - Xisang Plateau: Palaeontology of Xisang, v. 4, p. 51–80 [in Chinese with English abstract].
- Zhang, B., 1986, Early Cretaceous orbitolinids from Xainza and Baingoin, Xisang: Bulletin of the Nanjing Institute of Geology and Palaeontology, Academia Sinica, v. 8, p. 101–121 [in Chinese with English abstract].
- Zhang, B., 1991, Cretaceous larger foraminifera orbitolines from Ngari, Western Xizang (Tibet) in Sun, D. L. et al. (eds.), Stratigraphy and palaeontology of Permian, Jurassic and Cretaceous from the Rutog region, Xizang (Tibet): Nanjing University Press, Nanjing, p. 68–87 (in Chinese with English abstract).
- Zhang, K. J., 2000, Cretaceous palaeogeography of Tibet and adjacent areas (China), Tectonic implications: Cretaceous Research, v. 21, p. 23–33.

- Zhang, K. J., Xia, B. D., Wang, G. M., Li, Y. T., and Ye, H. F., 2004, Early Cretaceous stratigraphy, depositional environments, sandstone provenance, and tectonic setting of central Tibet, western China: Geological Society of America Bulletin, v. 116, p. 1202–1222.
- Zhu, D. C., Mo, X. X., Niu, Y. L., Zhao, Z. D., Wang, L. Q., Liu, Y. S., and Wu, F. Y., 2009, Geochemical investigation of Early Cretaceous igneous rocks along an east-west traverse throughout the central Lhasa Terrane, Tibet: Chemical Geology, v. 268, p. 298–312.
- Zhu, D. C., Zhao, Z. D., Niu, Y. L., Mo, X. X., Chung, S. L., Hou, Z. Q., Wang, L. Q., and Wu, F. Y., 2011, The Lhasa Terrane: Record of a microcontinent and its histories of drift and growth: Earth and Planetary Science Letters, v. 301, p. 241–255.
- Zhu, D. C., Zhao, Z. D., Niu, Y. L., Dilek, Y., Hou, Z. Q., and Mo, X. X., 2013, The origin and pre-Cenozoic evolution of the Tibetan Plateau: Gondwana Research, v. 23, p. 1429–1454.

Received 7 March 2016
Accepted 30 November 2016